

---

# Modular Multimodal Classification Without Fine-Tuning: A Simple Compositional Approach

---

Herman Bergström<sup>\*†1,2</sup> Aditya Mehrotra<sup>\*2,3</sup> Rahul G. Krishnan<sup>2,3</sup>

<sup>1</sup>Chalmers University of Technology and University of Gothenburg

<sup>2</sup>Vector Institute <sup>3</sup>University of Toronto

hermanb@chalmers.se aditmeh@cs.toronto.edu

## Abstract

We introduce CoMET, *Composing Modality Encoders with Tabular foundation models*, a simple yet highly competitive method for multimodal classification: pass each modality through a frozen pre-trained backbone, compress the resulting embeddings with PCA, and concatenate as input into a Tabular Foundation Model (TFM) for prediction. We show that PCA alone suffices to act as an adaptor yielding strong, robust performance across modalities. When the CLS tokens of the foundation model align poorly with downstream tasks, we propose **PALPooling**, a lightweight adaptive token pooler that consistently improves representation quality. By composing strong frozen representation learning backbones with TFMs, our approach achieves state-of-the-art results across diverse multimodal benchmarks without any training. On hierarchical tasks with large fine-grained class spaces, our approach enables fast and scalable classification, handling datasets with over 500,000 samples and 2,000 classes without any fine-tuning. Overall, our results show that the composition of foundation models is a simple, yet powerful, out-of-the-box solution for multimodal learning, challenging the necessity of complex, end-to-end training pipelines for new problems.

## 1 Introduction

Tabular Foundation Models (TFMs) have recently demonstrated that strong predictive performance can be achieved by amortizing Bayesian inference via in-context learning (Qu et al., 2025; Hollmann et al., 2022; Ma et al., 2024). After pre-training, these models can be applied to new datasets without additional fine-tuning, avoiding the substantial training times that come with task-specific pipelines. Surprisingly, despite being trained on priors designed to mimic the data-generating process observed in tabular data, the models are effectively data-agnostic. Instead, we find that, by applying simple dimensionality reduction techniques, TFMs become competitive classification heads for representations extracted using modality-specific encoders, such as image and text (see section 5).

This unexpected modality agnosticism raises a natural question: Can TFMs be used for fine-tuning-free multimodal classification? While there is limited initial work leveraging TFMs in multimodal setups, these either employ dataset-specific fine-tuning (Kim et al., 2026), or treat them as tabular encoders operating solely on tabular data (Luo et al., 2025). We argue that this not only detracts from the out-of-the-box nature of these models, but it is also not necessary to achieve competitive performance. Instead, we propose solving the task as a simple composition of foundation models, leveraging pre-trained encoders (Siméoni et al., 2025; Clark et al., 2020) for non-tabular features, and a TFM to make the final predictions, a modular pipeline where components can be independently replaced or extended without retraining.

---

\*Equal contribution. †Work was performed while at the University of Toronto.

Despite this simplicity, a potential bottleneck emerges in the interface between modality encoders and TFMs. In practice, representations are typically obtained via fixed pooling strategies, such as CLS-tokens or mean-pooling (Dosovitskiy et al., 2020; Devlin et al., 2019). When these embeddings fail to prioritize features relevant to the classification task, the final prediction quality may be limited, even when the backbone and TFM are individually strong. While adaptive pooling of individual tokens can traditionally help alleviate this issue (Reimers and Gurevych, 2019b), this would require fine-tuning, which in our setting would entail backpropagation through the TFM. To address this, we introduce Pseudo Attention Label Pooling (PALPooling). PALPooling is a lightweight pooling method that can be fit in seconds using one to three forward passes, preserving the training-free pipeline while enabling adaptive pooling in settings where backpropagation is not possible.

In this work, we make the following contributions. **i)** We demonstrate that reducing the embedding dimensionality through PCA is enough to make TabICL a competitive multimodal classifier, without any further fine-tuning. **ii)** Given this finding, we propose **CoMET**, *Composing Modality Encoders with Tabular foundation models*, an easy-to-implement framework offering high classification accuracy with minimal implementation effort. **iii)** We introduce PALPooling, an adaptive pooling method that uses pseudo-attention labels to avoid backpropagation. The method demonstrates benefits for both image and text settings, outperforming CLS tokens that are misaligned with the target prediction, with minimal computational overhead. **iv)** We highlight that strong fine-tuning-free classification enables new applications, showcasing this in the setting of hierarchical prediction.

## 2 Related Work

**Tabular Foundation Models** Prior-fitted networks were introduced by Müller et al. (2021), and have since paved the way for a new approach to generalizable tabular foundation models (Hollmann et al., 2022). The typical approach, employed by models like TabPFN (Hollmann et al., 2025) and TabICL (Qu et al., 2025), entails fitting the posterior predictive distribution on extensive synthetically generated data. However, models such as TabDPT (Ma et al., 2024) show that competitive performance can be achieved when using large amounts of real-world data for the prior. While these TFMs were originally limited to small datasets with few features, recent iterations have begun to relax these constraints (Qu et al., 2026; Grinsztajn et al., 2025). Although the focus of this paper is to showcase the proof of concept, we anticipate that the underlying framework will naturally extend to other tasks such as causal effect estimation Balazadeh et al. (2025).

**Multimodal Classification** While there is extensive work exploring architectures that can efficiently integrate tabular features with other modalities, these often focus on a single non-tabular modality at a time. Bonnier (2024) propose TTT, a Tabular Text Transformer which constructs embedding vectors through a distance-to-quantile mechanism, but requires dataset-specific fine-tuning. TabSTAR (Arazi et al., 2025) is closer to a pre-trained foundation model, but still requires a small amount of dataset-specific fine-tuning using Low Rank Adaptations (Hu et al., 2022). Another line of research utilizes contrastive learning between tabular and image features to learn joint representations, with models such as TIP (Du et al., 2024) and MMCL (Hager et al., 2023). Still, these models require end-to-end fine-tuning on a per-dataset basis.

**Tabular Foundation Models on Multimodal Data** TIME (Luo et al., 2025) uses TabPFN to extract representations for the tabular features, and subsequently fuses these with image features (e.g., through concatenation) before training a linear classifier on top. Perhaps most similar to our setting, the recently proposed MMPFN (Kim et al., 2026), which forwards image and text features through the TabPFN backbone, but crucially employs fine-tuning with modality-specific projectors and a tabular alignment loss. As we show in Section 6.2, this is not required, and we outperform their model using simple dimensionality reduction and TabICLv2.

## 3 Background

Transformer-based foundation models have learned to encode rich structure across different data modalities (Mur-Labadia et al., 2026; Siméoni et al., 2025; Clark et al., 2020), outputting contextualized token embeddings. Concretely, given an input from modality  $m$ , the backbone  $\Phi_m(\cdot)$  produces a set of token embeddings corresponding to modality-specific units (e.g., image patches or subword

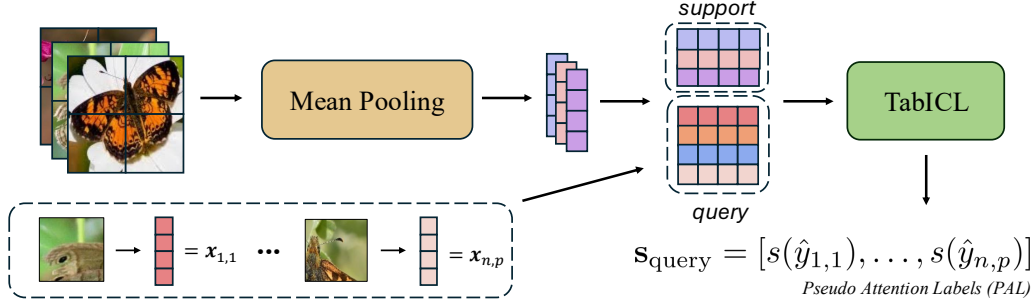


Figure 1: Construction of Pseudo Attention Labels. The support set comprises pooled text or image representations, whereas the query comprises more fine-grained tokens. The final PALs are produced by applying a scoring function,  $s(\cdot)$ , to the token-level predicted probability distributions.

tokens). To aggregate these tokens into a fixed-size representation suitable for downstream tasks, we typically leverage a pooling function, such as mean-pooling, learned attention-based pooling, or direct use of a dedicated classification (CLS)-token, a special token trained to summarize the input according to the model’s pre-training objective.

We focus on the task of multiclass classification. Formally, for a sample  $i$ , we wish to predict the class label  $y_i \in \{1, \dots, C\}$  based on features  $\mathbf{x}_i \in \mathbb{R}^d$ .  $\mathbf{x}_i$  can correspond to features from a single modality, or a concatenation of multiple (e.g.,  $\mathbf{x}_i = (\mathbf{x}_i^{\text{tab}}, \mathbf{x}_i^{\text{img}}, \mathbf{x}_i^{\text{text}})$ ). For any non-tabular modality, we leverage the encoders mentioned above to extract  $P$  local token embeddings  $\mathbf{X}_i^m \in \mathbb{R}^{P \times d_m}$ , and apply a pooling function,  $\text{Pool}(\mathbf{X}_i^m)$ , to construct summarized embeddings  $\mathbf{x}_i^m \in \mathbb{R}^{d_m}$ .

TFMs are amortized meta-learners (Qu et al., 2025; Liu and Ye, 2025), trained to predict the posterior predictive distribution over a set of *query* features, conditioned on a *support* set,  $\mathcal{D}_{\text{sup}} = \{(\mathbf{x}_1, y_1), \dots, (\mathbf{x}_n, y_n)\}$ . By training solely on synthetically generated data, they approximate  $\hat{y}_{\text{qry}} \approx P(y_{\text{qry}} | \mathbf{x}_{\text{qry}}, \mathcal{D}_{\text{sup}})$ , where  $\hat{y}_{\text{qry}} \in [0, 1]^C$  corresponds to the predicted label distribution. While  $\mathcal{D}_{\text{sup}}$  and  $\mathcal{D}_{\text{qry}}$  will in many cases correspond to the training and evaluation sets, respectively, TFMs leverage the support set through in-context learning, meaning no parameters are tuned. Note that since we distinguish between token-level representations  $\mathbf{X}_i^m$  and pooled features  $\mathbf{x}_i^m$ , we let  $\mathcal{D}_{\text{sup}}$  correspond to pooled multimodal features by default, and use a superscript  $\mathcal{D}_{\text{sup}}^{m, \text{tok}} = \{\mathbf{X}_i^m, y_i\}_{i \in \mathcal{I}_{\text{sup}}}$ , when operating on modality-specific token level representations in Section 4.1.

## 4 Method

When making a multimodal prediction, the CoMET method works as follows: **1.** For each non-tabular modality, we extract sample-wise token-level embeddings  $\mathbf{X}_i^m$  using a frozen pre-trained backbone  $\Phi_m$ . **2.** Vector representations  $\mathbf{x}_i^m$  are constructed using a (potentially learned) pooling function  $\text{Pool}(\mathbf{X}_i^m)$ . **3.** We fit a PCA projection  $\mathbf{U}_m \in \mathbb{R}^{d_m \times \tilde{d}_m}$  on the pooled features in  $\mathcal{D}_{\text{sup}}$  (i.e., on  $\{\mathbf{x}_i^m\}_{i \in \mathcal{I}_{\text{sup}}}$ ), giving us the compressed modality-specific representations  $\tilde{\mathbf{x}}_i^m = \mathbf{U}_m^\top \mathbf{x}_i^m$ . **4.** The projected support set  $\tilde{\mathcal{D}}_{\text{sup}} = \{(\tilde{\mathbf{x}}_i, y_i)\}_{i \in \mathcal{I}_{\text{sup}}}$ , where  $\tilde{\mathbf{x}}_i = (\mathbf{x}_i^{\text{tab}}, \tilde{\mathbf{x}}_i^{m_1}, \dots, \tilde{\mathbf{x}}_i^{m_M})$ , is then passed to the TFM to make the final prediction,  $\hat{y}_{\text{qry}} = \text{TFM}(\tilde{\mathbf{x}}_{\text{qry}}, \tilde{\mathcal{D}}_{\text{sup}})$

### 4.1 PALPooling

Adaptive pooling of image and text tokens often outperforms relying on the CLS-token (Reimers and Gurevych, 2019b). Still, in our setting, traditional fine-tuning of such a layer would require backpropagation through a tabular foundation model, detracting from its off-the-shelf nature. To avoid this, we introduce Pseudo Attention Label Pooling (PALPooling). Inspired by the fact that a standard attention layer with one head and a learned query vector simplifies to linear scoring, PALPooling fits this linear model through ridge regression on token-level pseudo attention labels derived from the model output, as opposed to backpropagation.

---

**Algorithm 1** PALPooler Fitting

---

**Require:** Training dataset  $\mathcal{D}_{\text{train}}^{\text{tok}}$ , scoring function  $s(\cdot)$ , max queries  $q_{\text{max}}$ , l2 reg  $\lambda$ , temperature  $\tau$

- 1: Initialize parameters  $\hat{\theta} = \mathbf{0} \in \mathbb{R}^d$   $\triangleright$  Yields mean-pooling via softmax
- 2: Define weight generation:  $\mathbf{w}(\mathbf{x}_i; \hat{\theta}) := \text{softmax}(\mathbf{X}_i \hat{\theta}) \in \mathbb{R}^P$
- 3: Define pooling function:  $\text{Pool}(\mathbf{X}_i; \hat{\theta}) := \sum_{p=1}^P \mathbf{w}_p(\mathbf{X}_i; \hat{\theta}) \cdot \mathbf{x}_{i,p}$
- 4: **for**  $t = 1, \dots, 3$  **do**
- 5:  $\mathcal{D}_{\text{sup}}^{\text{tok}}, \mathcal{D}_{\text{qry}}^{\text{tok}} \leftarrow \text{RandomSplit}(\mathcal{D}_{\text{train}}, 0.5)$
- 6:  $\mathcal{D}_{\text{sup}} \leftarrow \left\{ \left( \text{Pool}(\mathbf{X}_i; \hat{\theta}), y_i \right) \right\}_{i \in \mathcal{I}_{\text{sup}}}$   $\triangleright$  Apply current pooler to support:  $\mathbb{R}^{\frac{n}{2} \times P \times d} \rightarrow \mathbb{R}^{\frac{n}{2} \times d}$
- 7:  $\mathbf{Z}_{\text{qry}} \leftarrow \text{Sample}(\text{Flatten}(\mathcal{D}_{\text{qry}}^{\text{tok}}), q_{\text{max}})$   $\triangleright$  Discard labels and flatten:  $\mathbb{R}^{\frac{n}{2} \times P \times d} \rightarrow \mathbb{R}^{q_{\text{max}} \times d}$
- 8:  $\hat{\mathbf{Y}}_{\text{qry}} \leftarrow \text{TFM}(\mathbf{Z}_{\text{qry}}, \mathcal{D}_{\text{sup}})$
- 9:  $\mathbf{s}_{\text{qry}} \leftarrow s(\hat{\mathbf{Y}}_{\text{qry}}) / \tau$
- 10:  $\hat{\theta} \leftarrow (\mathbf{Z}_{\text{qry}}^{\top} \mathbf{Z}_{\text{qry}} + \lambda \mathbf{I})^{-1} \mathbf{Z}_{\text{qry}}^{\top} \mathbf{s}_{\text{qry}}$   $\triangleright$  Closed-form Ridge Regression
- 11: **end for**
- 12: **return** Learned pooling parameters  $\hat{\theta}$

---

Formally, our goal is to learn a pooling function  $\text{Pool}(\cdot)$ , parameterized by a linear scoring vector  $\theta \in \mathbb{R}^d$ , which outputs a weighted average of token representations. To fit this model, we split the modality specific training set,  $\mathcal{D}_{\text{train}}^{m, \text{tok}}$ , into two distinct sets, pooling the first,  $\mathcal{D}_{\text{sup}}^{m, \text{tok}}$ , to construct our support and using the second,  $\mathcal{D}_{\text{qry}}^{m, \text{tok}}$ , as the query set of individual tokens for which we will derive Pseudo Attention Labels (PALs). These labels are constructed through a scoring function  $s(\cdot) : [0, 1]^C \rightarrow \mathbb{R}$ , that takes as input the predicted label distribution. For convenience, we drop the modality superscript  $m$  as the method is only applied to a single modality at a time. The flow is illustrated in Figure 1, the fitting is described in Algorithm 1<sup>2</sup>, and we discuss the scoring function  $s$  below. As demonstrated in Appendix 4.1, running PALPooling more than once, using the previously fitted pooler to refine the support, yields a positive impact; we therefore run this method iteratively.

Choosing the scoring function  $s$  is a crucial design choice for this method. We find that naive approaches, such as basing the score on the correct-class prediction probability or prediction entropy perform poorly on non-trivial datasets (see Figure 11 in Appendix). Instead, we find that the most stable solutions measure the distributional distance between the predictions and the prior label frequency in the dataset, motivated by the idea that tokens that move the prediction from the prior distribution are *generally* more informative. That is, let  $\bar{\mathbf{y}} \in [0, 1]^C$  be the empirical label frequency, then  $s(\hat{\mathbf{y}}_{i,p}) = \ln(\text{dist}(\hat{\mathbf{y}}_{i,p}, \bar{\mathbf{y}}))$ , where  $\text{dist}$  is some function measuring distributional distance/divergence. In practice, we find the Jensen-Shannon Divergence (JSD) (Lin, 2002) to work well due to its bounded nature. In addition to fitting a pooling layer in seconds, PALPooling can be employed in settings where backpropagation through the TFM is impossible.

## 5 Bridging TFMs and Non-Tabular Representations through PCA

We start by demonstrating the performance of TabICLv2 (Qu et al., 2026) as a general-purpose prediction head. TabICL is a suitable choice as it significantly alleviates many of the computational scaling issues of its peers. We perform experiments on image and text datasets, extracting image features using the CLS-token from DINOv3 (Siméoni et al., 2025), and text features through ELECTRA (Clark et al., 2020) with mean-pooling. Complete descriptions of the datasets can be found in Appendix A. In addition to comparing TabICL with classic probing baselines, we evaluate the performance of all methods after first reducing the embedding dimensionality to 256 through PCA. In this paper, we show that the benefits of PCA are two-fold:

1. **Applying PCA has a significant positive effect on TabICL’s image-only and text-only performance.** Figure 2 compares the performance of TabICL against linear probing and a two-layer MLP on image-only and text-only classification. By applying PCA, TabICL

---

<sup>2</sup>Note that in practice, we always fit PCA on the pooled support, but exclude this in the formalization for clarity.

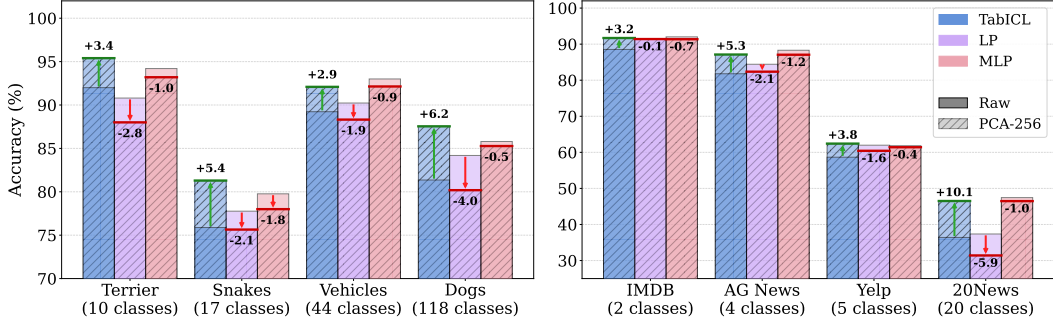


Figure 2: TabICL, Linear Probing (LP) and a 2-layer MLP with a ReLU activation evaluated on different datasets in text and image modalities with/without PCA. **Left:** Four subsets of ImageNet (described in Appendix A.2). **Right:** Four text classification datasets. Across both modalities, PCA substantially improves TabICL’s performance, enabling it to match or outperform the baselines.

achieves strong performance without any fine-tuning, often significantly outperforming linear probing. Importantly, the benefits of this projection do not extend to other classical probing heads, highlighting that TabICL’s improvements stem from changes in the geometry of the data rather than information content. Text and image representations are generally of low effective rank (Yin and Shen, 2018), and applying PCA significantly increases this. We investigate the relationship between this and TabICL’s prior in Appendix C.

2. **Applying PCA to extracted representations helps balance signals from tabular and non-tabular features.** In Figure 3, we run experiments on four datasets where the tabular features hold considerable signal: News Channel, Salary, PAD-UFES, and Petfinder. We find that PCA is crucial to avoid performance degradation in these settings.

The two benefits discussed here motivate why PCA is a crucial component in the CoMET setup. In Appendix B, we include results for TabPFNv2.5 (Grinsztajn et al., 2025), with and without PCA. We note that, while it achieves competitive performance, it becomes computationally expensive to run for larger datasets, especially in the many-class setting.

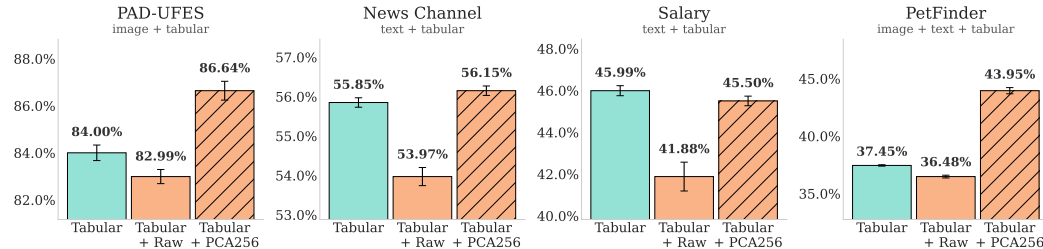


Figure 3: Accuracy on 4 datasets, where naively concatenating embeddings with tabular features deteriorates performance.

## 6 Experiments

### 6.1 Experimental Setup

To emphasize the simplicity of CoMET, we do not perform any hyperparameter tuning. Unless otherwise stated, we use ELECTRA ( $\Phi_{\text{text}}$ ) with mean-pooling, the CLS-token from DINOv3 ( $\Phi_{\text{img}}$ ), and a PCA dimension of 256 (see Appendix D.1 for an ablation). Additional information on all datasets used in the following experiments is provided in Appendix A.

**PALPooling** We first evaluate PALPooling in a unimodal setup, on both text and image datasets. Since texts vary in length, we employ a sample importance weight  $w_i = (\sqrt{\#\text{tokens}_i})^{-1}$  when fitting the ridge model to avoid overfitting the pooler to longer sequences. For  $\Phi_{\text{img}}$ , the number

of individual tokens is fixed. Still, the spatial structure of images allows us to do more coarse-grained pooling by first aggregating individual tokens in groups of, for example,  $2 \times 2$  or  $4 \times 4$  using local mean-pooling. We observe that sequentially increasing the granularity leads to stable convergence, while reducing the number of tokens processed in earlier iterations, and, as such, employ group sizes  $4 \times 4 \rightarrow 2 \times 2 \rightarrow 1 \times 1$  (see Appendix 4.1 for ablations). We run 3 iterations of pooling, with  $q_{max} = 5 \times 10^5$ ,  $\lambda = 10^4$ , and PCA dimension 128 for all experiments, with  $\tau = 0.5$  for image pooling and  $\tau = 1$  for text pooling. For images, we run experiments on 4 datasets where we expect the CLS-token to struggle due to the presence of multiple semantically meaningful objects/features in a given image, and only a subset of these are important for the classification. These are: Pneumonia (Shih et al., 2019), Butterflies (phuc, 2024), MS COCO (Lin et al., 2014), and Open Images (Kuznetsova et al., 2020). For texts, we evaluate on 4 popular datasets with varying text lengths, these are: IMDB Reviews (Maas et al., 2011), 20 Newsgroups (Lang, 1995), Yelp Reviews (Yelp, 2015), and AG News (Zhang et al., 2015). For robustness, we include results on a collection of ImageNet tasks where the main object is easy to discern in Appendix D. Here, we expect the CLS token to be strong, but show that PALPooling consistently outperforms mean pooling, the starting point of the algorithm.

Table 1: Dataset statistics of the datasets used for our multimodal results. Max seq. len is capped at the maximum ELECTRA token sequence length of 512. We subsample Jigsaw to 100,000/212,115 samples for train and 25,000/53,089 samples for test due to computational constraints.

Dataset	Train	Test	Tab. feats	Max seq. len	Image	Text	Tabular
WikiArt	57,010	24,434	2	—	✓		✓
PetFinder	8,791	5,861	9	512	✓	✓	✓
MM-IMDb	18,171	7,788	0	512	✓	✓	
Airbnb	15,794	6,769	50	512		✓	✓
Wine Reviews	84,123	21,031	4	194		✓	✓
Jigsaw Toxicity	100,000	25,000	29	358		✓	✓

**Multimodal Evaluation** We evaluate multimodal classification performance on datasets that mix tabular, text, and image data. An overview of the datasets is given in Table 1. We compare the performance of our compositional setup against standard baselines as well as SOTA multimodal frameworks. For *Text + Tabular* baselines we include TTT (Bonnier, 2024) and TabSTAR (Arazi et al., 2025), trained models that operate on raw tokens rather than mean-pooled ELECTRA embeddings. For *Image + Tabular* and *Image + Text + Tabular*, we include MMPFN (Kim et al., 2026), AutoGluon (Tang et al., 2024) and Catboost (Prokhorenkova et al., 2018). Recent work Ye et al. (2025) and Luo et al. (2025) has shown that TFMs can serve as powerful feature encoders of tabular data. Hence, we also include a Tabular Encoder (TE) baseline that extracts tabular embeddings using TabICL, concatenates them with the text/image embeddings, and then feeds the result into a 2-layer MLP. The tabular embeddings are constructed using the leave-one-out method from Ye et al. (2025).

## 6.2 Results

The results of the unimodal PALPooling experiments are shown in Table 2. While the magnitude of the performance gain varies across datasets and sizes, we observe that it can significantly increase accuracy with only a few seconds of additional overhead, with improvements most pronounced on Pneumonia and Butterflies. Figure 4 shows visualizations of the produced pseudo attention labels and the final learned pooling model. The Pneumonia results demonstrate that PALs can go beyond simple foreground-background separation, capturing finer-grained details such as the lung regions.

Table 3 reports the results of the multimodal experiments. Across nearly all datasets, CoMET matches or beats baselines, including MMPFN, the closest prior work that leverages TFMs for multimodal prediction. The notable exception is the Wine dataset, where TTT and TabSTAR outperform our approach. Both of these methods specialize in tabular+text data and operate at a finer granularity, consuming individual token embeddings directly instead of an aggregate, which could be beneficial for some tasks. The performance difference between CoMET and the TE method highlights the added benefit of not using TFMs as tabular-only encoders; instead, CoMET leverages their expressivity to enable richer cross-modal interactions.

Table 2: Unimodal PALPooling results on image (**left**) and text (**right**) datasets, averaged over 5 seeds. PAL accuracy is taken at the best-validation iteration; fit time is cumulative up to that iteration.

Dataset	$n_{train}$	CLS	Mean	PAL	Time	Dataset	$n_{train}$	CLS	Mean	PAL	Time
Pneumonia	20%	82.04 (0.07)	81.73 (0.23)	<b>82.95</b> (0.27)	16s	IMDB	20%	87.68 (0.19)	90.05 (0.21)	<b>90.23</b> (1.07)	1.0m
	100%	82.96 (0.02)	82.18 (0.00)	<b>83.73</b> (0.24)	48s		100%	89.10 (0.02)	91.02 (0.00)	<b>91.31</b> (0.61)	2.4m
Butterflies	20%	59.94 (1.67)	79.80 (0.71)	<b>84.68</b> (1.72)	8s	20 News	20%	28.09 (0.46)	36.09 (0.58)	<b>36.37</b> (1.03)	16s
	100%	76.80 (0.22)	90.28 (0.32)	<b>93.67</b> (0.53)	54s		100%	37.54 (0.02)	45.44 (0.00)	<b>46.67</b> (0.99)	1.7m
MS COCO	20%	88.95 (0.29)	91.55 (0.35)	<b>91.74</b> (0.24)	36s	Yelp	20%	66.02 (0.10)	68.07 (0.11)	<b>68.38</b> (0.42)	1.0m
	100%	91.60 (0.01)	93.74 (0.00)	<b>94.12</b> (0.03)	1.2m		100%	67.39 (0.00)	69.17 (0.00)	<b>69.81</b> (0.38)	1.8m
Open Images	20%	85.97 (0.15)	91.08 (0.14)	<b>91.59</b> (0.24)	43s	AG News	20%	78.89 (0.19)	83.20 (0.15)	<b>84.04</b> (0.33)	46s
	100%	88.69 (0.01)	93.07 (0.01)	<b>93.18</b> (0.03)	52s		100%	81.17 (0.01)	85.54 (0.00)	<b>85.94</b> (0.32)	1.4m



Figure 4: Example of PALs and the final pooling weights from the image datasets in Table 2. Top-left: Butterflies. Top-right: Pneumonia. Bottom-left: MS COCO. Bottom-right: Open Images.

The benefits of PALPooling vary across multimodal datasets, offering a boost on Jigsaw, Wine, and MM-IMDB, performing similarly on Airbnb, and performing worse on Petfinder. As previously discussed, we do not expect PALPooling to always outperform the CLS token, and its effectiveness will depend on the extent to which the CLS and mean-pooled representations fail to capture the signal. Furthermore, because the pooler is agnostic to features from other modalities, it is not necessarily emphasizing complementary information (see Figure 12 in Appendix D for example).

## 7 Fast and Accurate Predictions on Datasets with Hierarchical Labels

The setting of hierarchical classification, in which classes can be grouped into subcategories, is common in data across various modalities (Lewis et al., 2004; Bang et al., 2023; Jiang et al., 2022; Park et al., 2024). Given the robust performance of CoMET, we now explore this as an interesting application where strong training-free predictions can be readily leveraged. We argue that the use of TFMs is motivated in this setting for two reasons: Firstly, when predicting subcategories further down the hierarchy, it is possible to remove uninteresting samples from the support sets, making them increasingly tailored to their specific task. Secondly, since TFMs are training-free, this so-called local approach (Zangari et al., 2024) can be leveraged without training separate models for each subtask, making it a feasible and computationally efficient approach for large hierarchies. We refer to this hierarchical inference model as H-CoMET, and describe it in Figure 5. We compare this method to Flat-CoMET (F-CoMET) and a 2-layer MLP (F-MLP), both of which predict the leaf nodes directly, without using a hierarchy. For computational feasibility, F-CoMET and H-CoMET

Table 3: Accuracy on multimodal datasets over 5 seeds. Best result per dataset is shown in **bold**. PF = PetFinder. For WikiArt and Wine, we randomly subsample to 10 classes per seed since MM-PFN only supports datasets with at most 10 classes (see Appendix B.1). T=Text, t=Tabular and I=Image.

	Dataset	CoMET + PAL	CoMET	TE	Auto Gluon	Cat Boost	MM-PFN	TTT	Tab-STAR
$T + t$	Jigsaw	95.25 (0.03)	94.72 (0.04)	94.74 (0.02)	94.73 (0.03)	94.75 (0.03)	94.21 (0.01)	95.68 (0.08)	<b>95.94</b> ( <b>0.14</b> )
	Wine	83.18 (1.85)	82.54 (1.81)	78.85 (2.04)	79.89 (1.84)	78.04 (2.05)	71.14 (1.73)	88.80 (2.81)	<b>90.79</b> ( <b>2.63</b> )
	Airbnb	45.15 (0.23)	<b>45.17</b> ( <b>0.24</b> )	43.87 (0.36)	39.89 (0.51)	38.97 (0.23)	43.12 (0.21)	37.57 (0.48)	40.52 (0.33)
	PF-Text	42.78 (0.07)	<b>43.26</b> ( <b>0.17</b> )	36.49 (0.08)	40.53 (0.19)	39.20 (0.35)	38.29 (0.22)	36.46 (0.31)	38.19 (0.50)
$I + t$	WikiArt	<b>89.04</b> ( <b>1.17</b> )	89.01 (1.23)	84.49 (1.81)	82.95 (1.69)	82.59 (1.57)	81.42 (0.45)	—	—
	PF-Img	40.46 (0.26)	<b>41.22</b> ( <b>0.15</b> )	38.05 (0.13)	39.54 (0.01)	37.50 (0.22)	39.94 (0.21)	—	—
$I + T + t$	PF-All	42.60 (0.29)	<b>44.38</b> ( <b>0.24</b> )	38.14 (0.19)	41.68 (0.00)	40.14 (0.48)	40.48 (0.28)	—	—
$I + T$	MM-IMDb	<b>63.95</b> ( <b>0.37</b> )	63.62 (0.20)	54.89 (0.01)	63.52 (0.20)	62.79 (0.34)	—	—	—

have a max support budget of 200,000 for any problem/subproblem. F-MLP uses 90% of the *full* training set for fitting, and 10% for model selection.

**Evaluation** We evaluate the performance of our hierarchical approach on a combination of text, image, and tabular data. Specifically, to first highlight the competitiveness of H-CoMET, we evaluate on the text benchmarks and baseline results provided by Zangari et al. (2024)<sup>3</sup>. The datasets include Amazon Reviews (Hou et al., 2024), Web of Science (WOS) (Kowsari et al., 2017) (CC BY 4.0), and Linux Bugs (Lyubinetz et al., 2018) (CC BY 4.0), and the baselines MATCH (Zhang et al., 2021), HiAGM (Zhou et al., 2020), HBGL (Jiang et al., 2022), GACaps (Bang et al., 2023), and a standard fine-tuned flat BERT model (Devlin et al., 2019). We refer to Zangari et al. (2024) for a thorough description of these. While the baselines are often fine-tuned end-to-end, we instead rely on a fixed backbone and pooling method for each dataset. More precisely, we use SentenceBERT (Reimers and Gurevych, 2019a) for Amazon Reviews and CodeBERT (Feng et al., 2020) for Bugs, and aggregate both using mean-pooling. Given its strong performance in Zangari et al. (2024), we use TF-IDF (Sparck Jones, 1972) followed by chi-squared feature selection for WOS, resulting in a similar dimensionality of 768. Since CoMET is a multimodal method, we additionally derive two datasets of our own, with considerably vaster hierarchies, from INaturalist Horn et al.

(2018) (image + tabular), and a larger version of Amazon Reviews (Amazon MM), which includes more product features (image + text + tabular). We refer to Appendix A.7 for details. Table 4 provides

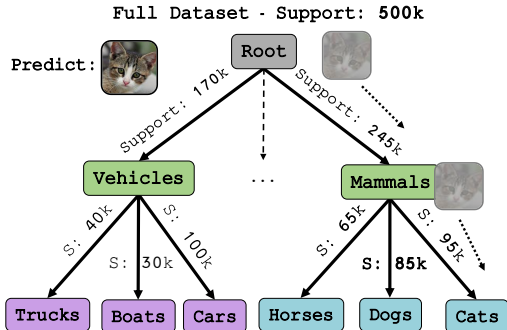


Figure 5: Hierarchical classification with CoMET. Given a broad classification problem, we construct a hierarchical tree in which the target classes reside at the leaf nodes and are grouped into higher-level categories represented by parent nodes. Each node defines a sub-classification problem over its children. We leverage TabICLv2 for each subproblem, constructing a fine-grained support by only including training samples from that category, and making the final predictions by traversing the hierarchy from root to leaf node, at each step forwarding the evaluation sample to the predicted node.

<sup>3</sup>Excluding multilabel and non- mandatory leaf node prediction datasets.

Table 4: Overview of the datasets used. Subtasks indicate the number of distinct TabICL supports used. Time refers to fitting + inference time for H-CoMET

Dataset	$n_{\text{train}}$	$n_{\text{test}}$	$n_{\text{classes}}$	Depth	Subtasks	Time
WOS	31k	16k	138	2	8	29s
Amazon	333k	167k	25	2	6	98s
Bugs	23k	12k	85	2	18	18s
iNaturalist	800k	28k	2895	7	1158	315s
Amazon MM	444k	55k	3047	4	633	310s

an overview of the dataset and the average execution time of H-CoMET, showing that performing inference with a TabICL classifier per-node finishes in a reasonable amount of time, even when the number of subtasks exceeds 1000.

**Results** The results in Table 5 emphasize the benefit of the hierarchical approach, with H-CoMET consistently outperforming F-CoMET, and reaching performance comparable to state-of-the-art hierarchical text models. The improvements are particularly pronounced on the Bugs dataset, with H-CoMET achieving significantly higher accuracy than baselines, owing to its ability to better handle the fine-grained subcategory classification (illustrated in Appendix D.4.2). H-CoMET also scales well to the more extensive multimodal Amazon MM and iNaturalist hierarchies, achieving high accuracy using 5 minutes of fitting and inference time. The F-MLP baseline still outperforms H-CoMET on iNaturalist, likely because it can better leverage the full 800k samples. Still, these results suggest that, as TFMs develop and become more scalable, their ability to handle large and complex hierarchical structures with a limited context length and no additional training holds great promise.

Table 5: Accuracy of H-CoMET, compared to our baselines and SOTA hierarchical text models.

Model	WOS $\uparrow$	Amazon $\uparrow$	Bugs $\uparrow$	Amazon MM $\uparrow$	iNaturalist $\uparrow$
MATCH	59.32 (1.61)	87.17 (0.87)	36.24 (4.91)	-	-
HiAGM	65.13 (1.59)	87.35 (0.44)	44.82 (0.69)	-	-
HBGL	<b>80.14 (0.02)</b>	84.05 (0.02)	57.63 (0.03)	-	-
GACaps	73.76 (0.78)	86.73 (0.19)	49.16 (0.52)	-	-
BERT	77.12 (0.67)	89.54 (0.20)	50.70 (1.13)	-	-
H-CoMET	75.53 (0.38)	<b>89.85</b> (0.04)	<b>76.61</b> (0.44)	<b>78.55</b> (0.06)	82.50 (0.04)
F-CoMET	73.41 (0.28)	87.17 (0.09)	31.44 (0.41)	73.19 (0.19)	69.54 (0.23)
F-MLP	76.16 (0.26)	88.48 (0.07)	31.40 (0.91)	77.15 (0.08)	<b>83.81</b> (0.09)

## 8 Conclusion

The results in this paper demonstrate the potential of composing strong modality encoders with in-context learners to make accurate predictions without task-specific fine-tuning. By balancing signals through PCA, CoMET achieves state-of-the-art performance on several multimodal benchmarks, despite the TFM never being explicitly trained on non-tabular data. As both TFMs and modality backbones improve, we anticipate that the gap between composing encoders with TFMs and fully trained end-to-end pipelines will continue to decrease. Longer context windows, larger class capacities, and richer pre-training priors may allow a single frozen compositional pipeline to ingest large databases of mixed-modality data and produce accurate predictions in seconds. More broadly, the modular nature of CoMET means it inherits future progress for free: new backbones or successor TFMs are drop-in upgrades, sidestepping the retraining and re-tuning that end-to-end pipelines typically require with each new release.

**Limitations and Future Work:** Our work is a first step, and several directions remain open. First, we relied on PCA as our adaptor between modality encoders and the TFM. While its simplicity is a start, more sophisticated TFM-informed dimensionality reduction methods could yield further gains without breaking the training-free pipeline. Furthermore, we focused on text and image modalities, but the same compositional template is general and extends naturally to any domain with strong

off-the-shelf encoders, such as audio, video, and 3D. We have shown that our compositional setup benefits complex data structures such as hierarchies; combined with the rise of agentic workflows, we see a natural path toward CoMET-driven structure discovery, where agents iteratively propose and evaluate organizations' data without any model retraining.

## **Acknowledgments**

RGK gratefully acknowledges support from the Canada Research Chairs Program (CRC-2022-00049) and the Canada CIFAR AI Chairs Program. This research was funded in part by a NFRF Special Call Award (NFRFR-2022-00526) and NSERC Discovery Grant (RGPIN-2022-04546). HB is supported by Swedish Research Council Grant 2022-04748, as well as the Sweden-America Foundation. Resources used in preparing this research were provided, in part, by the Province of Ontario, the Government of Canada through CIFAR, and companies sponsoring the Vector Institute.

## References

- Alan Arazi, Eilam Shapira, and Roi Reichart. Tabstar: A tabular foundation model for tabular data with text fields. *arXiv preprint arXiv:2505.18125*, 2025.
- John Arevalo, Tamar Solorio, Manuel Montes-y Gómez, and Fabio A. González. Gated multimodal units for information fusion. In *5th International Conference on Learning Representations (ICLR) Workshop*, 2017.
- Vahid Balazadeh, Hamidreza Kamkari, Valentin Thomas, Benson Li, Junwei Ma, Jesse C Cresswell, and Rahul G Krishnan. Causalpfn: Amortized causal effect estimation via in-context learning. *arXiv preprint arXiv:2506.07918*, 2025.
- Jinhyun Bang, Jonghun Park, and Jonghyuk Park. Gacaps-htc: graph attention capsule network for hierarchical text classification. *Applied Intelligence*, 53(17):20577–20594, 2023.
- Thomas Bonnier. Revisiting multimodal transformers for tabular data with text fields. In *Findings of the Association for Computational Linguistics: ACL 2024*, pages 1481–1500, 2024.
- Kevin Clark, Minh-Thang Luong, Quoc V Le, and Christopher D Manning. Electra: Pre-training text encoders as discriminators rather than generators. *arXiv preprint arXiv:2003.10555*, 2020.
- Jacob Devlin, Ming-Wei Chang, Kenton Lee, and Kristina Toutanova. Bert: Pre-training of deep bidirectional transformers for language understanding. In *Proceedings of the 2019 conference of the North American chapter of the association for computational linguistics: human language technologies, volume 1 (long and short papers)*, pages 4171–4186, 2019.
- Alexey Dosovitskiy, Lucas Beyer, Alexander Kolesnikov, Dirk Weissenborn, Xiaohua Zhai, Thomas Unterthiner, Mostafa Dehghani, Matthias Minderer, Georg Heigold, Sylvain Gelly, et al. An image is worth 16x16 words: Transformers for image recognition at scale. *arXiv preprint arXiv:2010.11929*, 2020.
- Siyi Du, Shaoming Zheng, Yinsong Wang, Wenjia Bai, Declan P O’Regan, and Chen Qin. Tip: Tabular-image pre-training for multimodal classification with incomplete data. In *European Conference on Computer Vision*, pages 478–496. Springer, 2024.
- Zhangyin Feng, Daya Guo, Duyu Tang, Nan Duan, Xiaocheng Feng, Ming Gong, Linjun Shou, Bing Qin, Ting Liu, Daxin Jiang, et al. Codebert: A pre-trained model for programming and natural languages. In *Findings of the association for computational linguistics: EMNLP 2020*, pages 1536–1547, 2020.
- Léo Grinsztajn, Klemens Flöge, Oscar Key, Felix Birkel, Philipp Jund, Brendan Roof, Benjamin Jäger, Dominik Safaric, Simone Alessi, Adrian Hayler, et al. Tabpfn-2.5: Advancing the state of the art in tabular foundation models. *arXiv preprint arXiv:2511.08667*, 2025.
- Paul Hager, Martin J. Menten, and Daniel Rueckert. Best of both worlds: Multimodal contrastive learning with tabular and imaging data. In *Proceedings of the IEEE/CVF Conference on Computer Vision and Pattern Recognition (CVPR)*, pages 23924–23935, June 2023.
- Noah Hollmann, Samuel Müller, Katharina Eggensperger, and Frank Hutter. Tabpfn: A transformer that solves small tabular classification problems in a second. *arXiv preprint arXiv:2207.01848*, 2022.
- Noah Hollmann, Samuel Müller, Lennart Purucker, Arjun Krishnakumar, Max Körfer, Shi Bin Hoo, Robin Tibor Schirrmeyer, and Frank Hutter. Accurate predictions on small data with a tabular foundation model. *Nature*, 637(8045):319–326, 2025.
- Grant Van Horn, Oisin Mac Aodha, Yang Song, Yin Cui, Chen Sun, Alex Shepard, Hartwig Adam, Pietro Perona, and Serge Belongie. The inaturalist species classification and detection dataset, 2018. URL <https://arxiv.org/abs/1707.06642>.
- Yupeng Hou, Jiacheng Li, Zhankui He, An Yan, Xiusi Chen, and Julian McAuley. Bridging language and items for retrieval and recommendation. *arXiv preprint arXiv:2403.03952*, 2024.

- Edward J Hu, Yelong Shen, Phillip Wallis, Zeyuan Allen-Zhu, Yuanzhi Li, Shean Wang, Liang Wang, Weizhu Chen, et al. Lora: Low-rank adaptation of large language models. *Iclr*, 1(2):3, 2022.
- Ting Jiang, Deqing Wang, Leilei Sun, Zhongzhi Chen, Fuzhen Zhuang, and Qinghong Yang. Exploiting global and local hierarchies for hierarchical text classification. In *Proceedings of the 2022 conference on empirical methods in natural language processing*, pages 4030–4039, 2022.
- Jigsaw and Conversation AI. Toxic comment classification challenge. <https://www.kaggle.com/c/jigsaw-toxic-comment-classification-challenge>, 2018.
- Wall Kim, Chaeyoung Song, and Hanul Kim. Multimodalpfn: Extending prior-data fitted networks for multimodal tabular learning. *arXiv preprint arXiv:2602.20223*, 2026.
- Kamran Kowsari, Donald E Brown, Mojtaba Heidarysafa, Kiana Jafari Meimandi, , Matthew S Gerber, and Laura E Barnes. Hdltext: Hierarchical deep learning for text classification. In *Machine Learning and Applications (ICMLA), 2017 16th IEEE International Conference on*. IEEE, 2017.
- Alina Kuznetsova, Hassan Rom, Neil Alldrin, Jasper Uijlings, Ivan Krasin, Jordi Pont-Tuset, Shahab Kamali, Stefan Popov, Matteo Mallocci, Alexander Kolesnikov, et al. The open images dataset v4: Unified image classification, object detection, and visual relationship detection at scale. *International journal of computer vision*, 128(7):1956–1981, 2020.
- Ken Lang. NewsWeeder: Learning to filter netnews. In *Machine Learning Proceedings 1995*, pages 331–339. Morgan Kaufmann, 1995. doi: 10.1016/B978-1-55860-377-6.50048-7.
- David D Lewis, Yiming Yang, Tony G Rose, and Fan Li. Rcv1: A new benchmark collection for text categorization research. *Journal of machine learning research*, 5(Apr):361–397, 2004.
- Jianhua Lin. Divergence measures based on the shannon entropy. *IEEE Transactions on Information theory*, 37(1):145–151, 2002.
- Tsung-Yi Lin, Michael Maire, Serge Belongie, James Hays, Pietro Perona, Deva Ramanan, Piotr Dollár, and C Lawrence Zitnick. Microsoft coco: Common objects in context. In *European conference on computer vision*, pages 740–755. Springer, 2014.
- Siyang Liu and Han-Jia Ye. Tabpfn unleashed: A scalable and effective solution to tabular classification problems. In *Forty-second International Conference on Machine Learning*, 2025.
- Yinhan Liu, Myle Ott, Naman Goyal, Jingfei Du, Mandar Joshi, Danqi Chen, Omer Levy, Mike Lewis, Luke Zettlemoyer, and Veselin Stoyanov. Roberta: A robustly optimized bert pretraining approach. *arXiv preprint arXiv:1907.11692*, 2019.
- Jiaqi Luo, Yuan Yuan, and Shixin Xu. Time: Tabpfn-integrated multimodal engine for robust tabular-image learning. *arXiv preprint arXiv:2506.00813*, 2025.
- Volodymyr Lyubinet, Taras Boiko, and Deon Nicholas. Automated labeling of bugs and tickets using attention-based mechanisms in recurrent neural networks. In *2018 IEEE Second International Conference on Data Stream Mining & Processing (DSMP)*, pages 271–275. IEEE, 2018.
- Junwei Ma, Valentin Thomas, Rasa Hosseinzadeh, Alex Labach, Hamidreza Kamkari, Jesse C Cresswell, Keyvan Golestan, Guangwei Yu, Anthony L Caterini, and Maksims Volkovs. Tabdpt: Scaling tabular foundation models on real data. *arXiv preprint arXiv:2410.18164*, 2024.
- Andrew Maas, Raymond E Daly, Peter T Pham, Dan Huang, Andrew Y Ng, and Christopher Potts. Learning word vectors for sentiment analysis. In *Proceedings of the 49th annual meeting of the association for computational linguistics: Human language technologies*, pages 142–150, 2011.
- Samuel Müller, Noah Hollmann, Sebastian Pineda Arango, Josif Grabocka, and Frank Hutter. Transformers can do bayesian inference. *arXiv preprint arXiv:2112.10510*, 2021.
- Lorenzo Mur-Labadia, Matthew Muckley, Amir Bar, Mido Assran, Koustuv Sinha, Mike Rabbat, Yann LeCun, Nicolas Ballas, and Adrien Bardes. V-jepa 2.1: Unlocking dense features in video self-supervised learning. *arXiv preprint arXiv:2603.14482*, 2026.

- Andre GC Pacheco, Gustavo R Lima, Amanda S Salomao, Breno Krohling, Igor P Biral, Gabriel G De Angelo, Fábio CR Alves Jr, José GM Esgario, Alana C Simora, Pedro BC Castro, et al. Pad-ufes-20: A skin lesion dataset composed of patient data and clinical images collected from smartphones. *Data in brief*, 32:106221, 2020.
- Seulki Park, Youren Zhang, Stella X Yu, Sara Beery, and Jonathan Huang. Visually consistent hierarchical image classification. *arXiv preprint arXiv:2406.11608*, 2024.
- PetFinder. Petfinder.my adoption prediction. <https://www.kaggle.com/c/petfinder-adoption-prediction>, 2019. Kaggle Competition Dataset.
- phuc. Butterfly image classification, 2024. URL <https://www.kaggle.com/datasets/phucthai02/butterfly-image-classification>. Accessed May 5, 2026.
- Liudmila Prokhorenkova, Gleb Gusev, Aleksandr Vorobev, Anna Veronika Dorogush, and Andrey Gulin. Catboost: unbiased boosting with categorical features. *Advances in neural information processing systems*, 31, 2018.
- Jingang Qu, David Holzmüller, Gaël Varoquaux, and Marine Le Morvan. TabICL: A tabular foundation model for in-context learning on large data. In *International Conference on Machine Learning*, 2025.
- Jingang Qu, David Holzmüller, Gaël Varoquaux, and Marine Le Morvan. TabICLv2: A better, faster, scalable, and open tabular foundation model. *arXiv preprint arXiv:2602.11139*, 2026.
- Nils Reimers and Iryna Gurevych. Sentence-bert: Sentence embeddings using siamese bert-networks. In *Proceedings of the 2019 Conference on Empirical Methods in Natural Language Processing*. Association for Computational Linguistics, 11 2019a. URL <http://arxiv.org/abs/1908.10084>.
- Nils Reimers and Iryna Gurevych. Sentence-bert: Sentence embeddings using siamese bert-networks. In *Proceedings of the 2019 conference on empirical methods in natural language processing and the 9th international joint conference on natural language processing (EMNLP-IJCNLP)*, pages 3982–3992, 2019b.
- Babak Saleh and Ahmed Elgammal. Large-scale classification of fine-art paintings: Learning the right metric on the right feature. *arXiv preprint arXiv:1505.00855*, 2015.
- Xingjian Shi, Jonas Mueller, Nick Erickson, Mu Li, and Alexander J. Smola. Benchmarking multimodal AutoML for tabular data with text fields. In *Proceedings of the Neural Information Processing Systems Track on Datasets and Benchmarks*, 2021.
- George Shih, Carol C Wu, Safwan S Halabi, Marc D Kohli, Luciano M Prevedello, Tessa S Cook, Arjun Sharma, Judith K Amorosa, Veronica Arteaga, Maya Galperin-Aizenberg, et al. Augmenting the national institutes of health chest radiograph dataset with expert annotations of possible pneumonia. *Radiology: Artificial Intelligence*, 1(1):e180041, 2019.
- Oriane Siméoni, Huy V Vo, Maximilian Seitzer, Federico Baldassarre, Maxime Oquab, Cijo Jose, Vasil Khalidov, Marc Szafraniec, Seungeun Yi, Michaël Ramamonjisoa, et al. Dinov3. *arXiv preprint arXiv:2508.10104*, 2025.
- Karen Sparck Jones. A statistical interpretation of term specificity and its application in retrieval. *Journal of documentation*, 28(1):11–21, 1972.
- Zhiqiang Tang, Haoyang Fang, Su Zhou, Taojiannan Yang, Zihan Zhong, Tony Hu, Katrin Kirchhoff, and George Karypis. Autogluon-multimodal (automm): Supercharging multimodal automm with foundation models. *arXiv preprint arXiv:2404.16233*, 2024.
- Zackary Thoutt. Wine reviews. <https://www.kaggle.com/datasets/zynicide/wine-reviews>, 2017.
- Shashanka Venkataramanan, Valentinos Pariza, Mohammadreza Salehi, Lukas Knobel, Spyros Gidaris, Elias Ramzi, Andrei Bursuc, and Yuki M. Asano. Franca: Nested matryoshka clustering for scalable visual representation learning. *arXiv preprint arXiv:2507.14137*, 2025.

- Han-Jia Ye, Si-Yang Liu, and Wei-Lun Chao. A closer look at tabpfn v2: Understanding its strengths and extending its capabilities, 2025. URL <https://arxiv.org/abs/2502.17361>.
- Yelp. Yelp open dataset. <https://www.yelp.com/dataset>, 2015. Yelp Dataset Challenge.
- Zi Yin and Yuanyuan Shen. On the dimensionality of word embedding. *Advances in neural information processing systems*, 31, 2018.
- Alessandro Zangari, Matteo Marcuzzo, Matteo Rizzo, Lorenzo Giudice, Andrea Albarelli, and Andrea Gasparetto. Hierarchical text classification and its foundations: A review of current research. *Electronics*, 13(7):1199, 2024.
- Xiang Zhang, Junbo Zhao, and Yann LeCun. Character-level convolutional networks for text classification. *Advances in neural information processing systems*, 28, 2015.
- Yu Zhang, Zhihong Shen, Yuxiao Dong, Kuansan Wang, and Jiawei Han. Match: Metadata-aware text classification in a large hierarchy. In *Proceedings of the Web Conference 2021*, pages 3246–3257, 2021.
- Jie Zhou, Chunping Ma, Dingkun Long, Guangwei Xu, Ning Ding, Haoyu Zhang, Pengjun Xie, and Gongshen Liu. Hierarchy-aware global model for hierarchical text classification. In *Proceedings of the 58th annual meeting of the association for computational linguistics*, pages 1106–1117, 2020.

## A Datasets & Experimental Details

### A.1 Compute Resources

We use a private compute cluster for our experiments. All CoMET experiments were conducted on L40s GPUs on nodes with 64-256GB of RAM. H100s with 256GB RAM were used to compute results with MM-PFN and TabPFNv2.5.

### A.2 ImageNet Subsets

In this paper we use subsets of ImageNet for image classification tasks. Our subsets along with their corresponding classes within each subset are detailed in Table 7.

Table 6

Dataset	Train	Val	Classes
Terrier	12,608	500	10
Snakes	21,871	850	17
Beetle	10,400	400	8
Feline	13,000	500	10
Vehicles	56,956	2,200	44
Dogs	147,873	5,900	118

### A.3 Text-only datasets

- **IMDB** Maas et al. (2011) consists of movie reviews represented using ELECTRA mean-pooled embeddings. The task is binary sentiment classification (positive vs. negative).
- **20 Newsgroups** Lang (1995) consists of newsgroup posts represented using ELECTRA mean-pooled embeddings. The task is topic classification over 20 classes.
- **AG News** Zhang et al. (2015) consists of news article titles and descriptions concatenated and represented using ELECTRA mean-pooled embeddings. The task is news-category classification over 4 classes: World, Sports, Business, and Sci/Tech.
- **Yelp** (Yelp Dataset Agreement) Zhang et al. (2015) consists of business reviews represented using ELECTRA mean-pooled embeddings. We sample 30,000 training examples and 10,000 test examples stratified by star rating. The task is review-rating classification over 5 classes.

The train/val splits and sequence lengths are outlined in Table 8. All texts are truncated to 512 tokens, which is ELECTRA’s maximum sequence length.

### A.4 Butterflies and RSNA Pneumonia

The Radiological Society of North America (RSNA) Pneumonia Detection dataset (Shih et al., 2019) consists of chest X-ray images annotated for the presence of pneumonia. It consists of 21,348 training images (16,572/4,776 positive/negative) and 5,336 test (4,100/1,236 positive/negative).

In contrast, the Butterfly Image Classification dataset (CC0 1.0) from Kaggle (phuc, 2024) contains high-resolution images of various butterfly species across multiple classes, designed for fine-grained visual categorization. We split into 5,200 train and 1,299 test, and the exact label distribution can be seen in Table 9.

Table 7: ImageNet subsets used in our experiments and their constituent classes.

Subset	Class Names
Terrier	Staffordshire bullterrier, American Staffordshire terrier, Bedlington terrier, Border terrier, Kerry blue terrier, Irish terrier, Norfolk terrier, Norwich terrier, Yorkshire terrier, wire-haired fox terrier.
Snakes	thunder snake, ringneck snake, hognose snake, green snake, king snake, garter snake, water snake, vine snake, night snake, boa constrictor, rock python, Indian cobra, green mamba, sea snake, horned viper, diamondback, sidewinder.
Beetle	tiger beetle, ladybug, ground beetle, long-horned beetle, leaf beetle, dung beetle, rhinoceros beetle, weevil.
Feline	tabby, tiger cat, Persian cat, Siamese cat, Egyptian cat, cougar, lynx, leopard, snow leopard, jaguar.
Vehicles	ambulance, amphibian, beach wagon, cab, convertible, fire engine, garbage truck, go-kart, golfcart, jeep, aircraft carrier, canoe, catamaran, container ship, fireboat, gondola, lifeboat, liner, pirate, schooner, airliner, airship, ashcan, electric guitar, forklift, jinrikisha, limousine, minivan, Model T, motor scooter, passenger car, racer, space shuttle, speedboat, sports car, steam locomotive, streetcar, tow truck, tractor, trailer truck, tricycle, unicycle, warplane, wing.
Dogs	Chihuahua, Japanese spaniel, Maltese dog, Pekinese, Shih-Tzu, Blenheim spaniel, papillon, toy terrier, Rhodesian ridgeback, Afghan hound, basset, beagle, bloodhound, bluetick, black-and-tan coonhound, Walker hound, English foxhound, redbone, borzoi, Irish wolfhound, Italian greyhound, whippet, Ibizan hound, Norwegian elkhound, otterhound, Saluki, Scottish deerhound, Weimaraner, Staffordshire bullterrier, American Staffordshire terrier, Bedlington terrier, Border terrier, Kerry blue terrier, Irish terrier, Norfolk terrier, Norwich terrier, Yorkshire terrier, wire-haired fox terrier, Lakeland terrier, Sealyham terrier, Airedale, cairn, Australian terrier, Dandie Dinmont, Boston bull, miniature schnauzer, giant schnauzer, standard schnauzer, Scotch terrier, Tibetan terrier, silky terrier, soft-coated wheaten terrier, West Highland white terrier, Lhasa, flat-coated retriever, curly-coated retriever, golden retriever, Labrador retriever, Chesapeake Bay retriever, German short-haired pointer, vizsla, English setter, Irish setter, Gordon setter, Brittany spaniel, clumber, English springer, Welsh springer spaniel, cocker spaniel, Sussex spaniel, Irish water spaniel, kuvasz, schipperke, groenendael, malinois, briard, kelpie, komondor, Old English sheepdog, Shetland sheepdog, collie, Border collie, Bouvier des Flandres, Rottweiler, German shepherd, Doberman, miniature pinscher, Greater Swiss Mountain dog, Bernese mountain dog, Appenzeller, EntleBucher, boxer, bull mastiff, Tibetan mastiff, French bulldog, Great Dane, Saint Bernard, Eskimo dog, malamute, Siberian husky, dalmatian, affenpinscher, basenji, pug, Leonberg, Newfoundland, Great Pyrenees, Samoyed, Pomeranian, chow, keeshond, Brabancon griffon, Pembroke, Cardigan, toy poodle, miniature poodle, standard poodle, Mexican hairless.

Table 8: Text classification datasets with their train/test splits, number of classes, and maximum sequence lengths.

Dataset	Train	Test	Classes	Max seq. len	Avg. seq. len
IMDB	25,000	25,000	2	512	273
20 NewsGroups	11,314	7,532	20	512	175
AG News	120,000	7,600	4	256	53
Yelp	30,000	10,000	5	512	129

Table 9: Object classes and their respective image counts in the train and test sets.

Class	Train	Test	Class	Train	Test
Adonis	73	15	African Giant Swallowtail	56	19
American Snoot	62	12	An 88	75	10
Appollo	70	20	Atala	83	17
Banded Orange Heliconian	78	19	Banded Peacock	68	15
Beckers White	63	18	Black Hairstreak	67	18
Blue Morpho	59	16	Blue Spotted Crow	74	12
Brown Siproeta	73	26	Cabbage White	72	18
Cairns Birdwing	68	15	Chequered Skipper	75	20
Chestnut	65	20	Cleopatra	76	17
Clodius Parnassian	70	17	Clouded Sulphur	69	23
Common Banded Awl	67	20	Common Wood-Nymph	76	14
Copper Tail	76	18	Crecent	80	17
Crimson Patch	63	9	Danaid Eggfly	72	22
Eastern Coma	72	21	Eastern Dapple White	71	21
Eastern Pine Elfin	70	25	Elbowed Pierrot	66	16
Gold Banded	60	13	Great Eggfly	62	16
Great Jay	77	17	Green Celled Cattleheart	68	20
Grey Hairstreak	67	19	Indra Swallow	64	17
Iphiclus Sister	71	24	Julia	66	15
Large Marble	66	15	Malachite	61	12
Mangrove Skipper	70	17	Mestra	73	13
Metalmark	64	12	Milberts Tortoiseshell	80	16
Monarch	66	24	Mourning Cloak	96	35
Orange Oakleaf	70	17	Orange Tip	76	20
Orchard Swallow	59	17	Painted Lady	69	9
Paper Kite	74	16	Peacock	68	16
Pine White	67	19	Pipevine Swallow	58	26
Popinjay	66	19	Purple Hairstreak	60	19
Purplish Copper	74	18	Question Mark	51	26
Red Admiral	68	14	Red Cracker	69	27
Red Postman	68	21	Red Spotted Purple	68	18
Scarce Swallow	81	16	Silver Spot Skipper	70	13
Sleepy Orange	85	22	Sootywing	72	18
Southern Dogface	76	11	Straited Queen	72	15
Tropical Leafwing	71	12	Two Barred Flasher	69	7
Ulyses	63	21	Viceroy	69	12
Wood Satyr	60	11	Yellow Swallow Tail	61	14
Zebra Long Wing	66	10			

## A.5 Multimodal datasets

- **Jigsaw Toxicity** (CC0 1.0) Jigsaw and Conversation AI (2018) consists of online comments paired with 24 demographic identity attributes and 5 user-engagement signals as tabular features, together with ELECTRA embeddings of the comment text. The task is binary toxicity classification.
- **Wine Reviews** (CC BY-NC-SA 4.0) Thoutt (2017) consists of wine descriptions paired with structured metadata — country, province, points, and price — as tabular features, together with ELECTRA embeddings of the review text. The task is variety classification over 20 classes.

- **WikiArt** Saleh and Elgammal (2015) consists of artwork images represented using DINOv3 embeddings, with no accompanying tabular or text features. The task is artistic-style classification over 27 classes.
- **PetFinder** PetFinder (2019) consists of pet adoption profiles with 12 structured tabular features, DINOv3 image embeddings, and ELECTRA embeddings of the pet description. The task is adoption-speed prediction over 5 classes.
- **MM-IMDb** Arevalo et al. (2017) consists of movie entries with DINOv3 poster-image embeddings and ELECTRA plot-synopsis embeddings, with no tabular features. The task is genre classification over 23 classes.
- **Airbnb** (CC BY-NC-SA 4.0) Shi et al. (2021) consists of Melbourne Airbnb listings with 23 categorical and 23 numerical tabular features, together with ELECTRA embeddings of the listing name, summary, and description. Following TTT Bonnier (2024), the nightly price is discretized into ten quantile-based classes.
- **PAD-UFES-20** (CC BY 4.0) Pacheco et al. (2020) consists of smartphone-captured skin-lesion images represented using DINOv3 embeddings, paired with 21 clinical tabular features including patient age, lesion diameter, anatomical region, skin type, and medical history. The task is lesion classification over 6 classes.
- **Salary India** (CC BY-NC-SA 4.0) Shi et al. (2021) consists of data scientist job postings with 5 structured tabular features — company, experience level, location, job designation, and job type — together with ELECTRA embeddings of the job description and key skills. The task is salary-range classification over 6 classes.
- **News Channel** (CC BY-NC-SA 4.0) Shi et al. (2021) consists of news articles with 16 numeric tabular features capturing NLP statistics and user-engagement signals, paired with ELECTRA embeddings of the article title. The task is channel classification over 6 classes.

## A.6 MS Coco & Open Images Task Construction

MS COCO (Lin et al., 2014) (CC BY 4.0) and Open Images (Kuznetsova et al., 2020) (CC BY 4.0 / CC BY 2.0) are originally object detection datasets, meaning a single image often has numerous labels associated with it. To construct a single-label dataset, we looked at the most commonly occurring labels, and removed images with co-occurrences. For MS Coco we did this by ignoring the "person" label, due to heavy co-occurrence with other labels, and then taking the 50 most commonly occurring labels. The final dataset consisted of 43 536 training samples and 31 335 test samples. The classes used, and their distribution, can be seen in Table 10. For Open Images, the process was similar, but since this dataset had a lot more fine-grained labels (e.g., Human arm), the list of ignored common labels (presented in Table 11b) needed to be substantially longer to avoid too many co-occurrences. The final dataset included 600 train and 200 test samples of each class, shown in Table 11a (30 000 /10 000 total).

## A.7 Amazon MM and iNaturalist dataset Preprocessing

The iNaturalist dataset contains 2.8M images. The hierarchy is severely unbalanced, so in order to avoid having the accuracy metrics be dominated by how well TabICL predicts the most popular branches we downsample it to 796,497 training images spanning 2,896 classes. To obtain a balanced hierarchy, we enforce that within each node, no child has more than a 4× smaller sample count than any other child. This is achieved through a bottom-up pruning procedure starting from the leaves, where low-sample nodes are iteratively pruned from the tree until the criterion is satisfied. The resulting tree is relatively well-balanced and suitable for benchmarking TabICL. We use six tabular features per image: *latitude*, *longitude*, *month\_sin*, *month\_cos*, *year*, and *location\_uncertainty*.

The Amazon MM dataset, derived from Amazon Reviews (Hou et al., 2024), includes the features listed in Table 12. Text features were extracted using Sentence-BERT on all texts concatenated. Image features were extracted using DINOv3. 9 top-level categories were used. These were: *Arts crafts and sewing*, *Automotive*, *Beauty and personal care*, *Cell phones and accessories*, *Clothing shoes and jewelry*, *Electronics*, *Home and kitchen*, *Sports and outdoors*, *Tools and home improvement*. We then take the following steps to clean and balance the dataset: We limit the depth to 4, and refer to the different levels as L0 (the 9 categories described above), L1, L2, and L3. We then drop L1

Table 10: Object classes and their respective image counts in the train and test sets.

Class	Train	Test	Class	Train	Test	Class	Train	Test
surfboard	2078	693	giraffe	1639	546	skis	1636	546
train	1469	490	skateboard	1462	487	airplane	1410	470
bird	1334	445	horse	1324	441	clock	1291	430
car	1054	352	boat	997	332	tie	964	322
toilet	921	307	dog	915	305	bench	799	266
motorcycle	790	263	tennis racket	735	245	cell phone	706	235
bed	626	208	cat	622	208	truck	598	200
bus	508	169	umbrella	505	168	traffic light	481	160
pizza	466	155	bowl	448	149	dining table	440	146
vase	427	142	sports ball	351	117	sink	350	116
backpack	317	106	handbag	311	104	bottle	300	100
baseball bat	284	94	chair	282	94	oven	268	89
baseball glove	262	87	cake	256	85	remote	220	73
cup	219	73	bicycle	214	71	laptop	184	62
tv	169	56	knife	160	54	book	142	47
potted plant	105	35	couch	98	32	fork	83	28
wine glass	58	20	spoon	57	19			

Beer	Bench	Bicycle	Man, Woman, Girl, Boy, Person; Human face, Human body, Human arm, Human hair, Human head, Human leg, Human mouth, Human eye, Human nose, Human hand, Human foot, Human ear, Human beard; Clothing, Footwear, Suit, Dress, Jeans, Hat, Shirt, Shorts, Glove, Coat, Sock, Tie, Swimwear, Trousers, Scarf, Fashion accessory; Sunglasses, Glasses, Mammal, Land vehicle; Vehicle, Furniture, Animal, Plant, Tree, Flower; Food, Drink, Building, House, Tower, Skyscraper; Wheel, Tire; Sports equipment, Auto part, Tableware, Musical instrument, Insect; Bicycle wheel, Vehicle registration plate; Jacket, Sports uniform, Goggles; Window, Door; Snack, Fast food, Baked goods, Dessert, Fruit, Vegetable; Bicycle helmet, Wine, Sun hat, Dairy Product, Ball (Object); Bookcase, Desk, Office building
Bird	Boat	Book	
Bottle	Bus	Butterfly	
Cake	Camera	Car	
Castle	Cat	Chair	
Coffee cup	Computer monitor	Dog	
Drum	Duck	Fish	
Fixed-wing aircraft	Flag	Flowerpot	
Football	Guitar	Helmet	
Horse	Houseplant	Laptop	
Microphone	Mobile phone	Motorcycle	
Palm tree	Picture frame	Poster	
Rose	Salad	Sculpture	
Shelf	Stairs	Street light	
Swimming pool	Table	Tent	
Toy	Train	Truck	
Van	Wine glass		

(a) Included Classes (50)

(b) Ignored common labels (66)

Table 11: Open Images class split

classes with fewer than 5000 items, L2 classes with fewer than 500, and L3 with fewer than 100. Additionally, we drop all L1 nodes that don't have any children, meaning the leaf-nodes are strictly located in L2 or L3. Within each parent node (subtask), we allow for a max class imbalance ratio of 5, subsampling larger classes until they are at most 5x the minority class.

Table 12: Product features of the Amazon MM dataset.

Name	Type
Title	Text
Description	Text
Features	Text
Product Image	Image
Price	Numeric
Rating	Numeric
Store	Categorical

## B Discussion on TabPFN

### B.1 MM-TabPFN’s class size limit

MM-PFN requires backpropogation through TabPFN to finetune its modality specific encoders. In its current form, TabPFN is not designed to perform backprop with more than 10 classes. There exists an extension to TabPFN called many-class-classifier that uses multiple evaluations of TabPFN at inference time, but not training, [https://github.com/PriorLabs/tabpfn-extensions/blob/main/examples/many\\_class/many\\_class\\_classifier\\_example.py](https://github.com/PriorLabs/tabpfn-extensions/blob/main/examples/many_class/many_class_classifier_example.py). Hence, we cannot evaluate the MM-PFN paper on large scale datasets with more than 10 classes.

### B.2 TabPFNV2.5 vs TabICLv2 on Unimodal datasets

In Figure 6, we find that TabPFNV2.5 performs slightly worse than TabICLv2 with PCA on image datasets, but matches TabICLv2 on text datasets. We also see that TabPFNV2.5 does not benefit from dimensionality reduction, compared to TabICLv2, which receives a significant boost in performance.

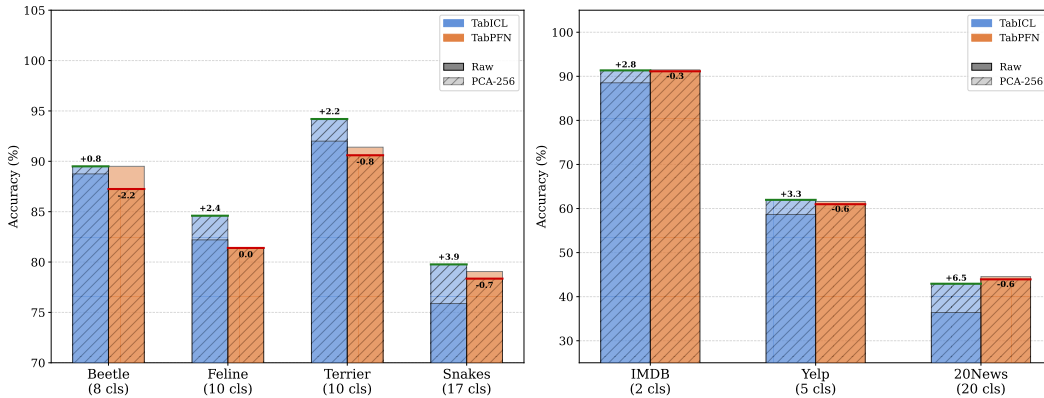


Figure 6: Performance of TabICL vs TabPFN on a few single modality datasets.

### B.3 TabPFNV2.5 vs TabICLv2 inference times

In Table 13, we compare inference times of TabICLv2 against TabPFNV2.5 on both raw CLS tokens and PCA versions. We find that TabICLv2 is significantly faster, showing that it’s a much better choice for large-scale multimodal datasets.

Table 13: Inference time for TabICL vs. TabPFN on a few single modality datasets. Lower is better.

Dataset	TabICL+CLS	TabICL+PCA	TabPFN+CLS	TabPFN+PCA
<i>ImageNet Subsets</i>				
Beetle (8 classes)	18 s	6 s	41 s	14 s
Feline (10 classes)	24 s	8 s	62 s	22 s
Terrier (10 classes)	23 s	8 s	60 s	21 s
Snakes (17 classes)	1.5 m	34 s	95 m	35 m
<i>Text</i>				
IMDB (2 classes)	31 m	12 m	2.9 h	52 m
Yelp (5 classes)	15 m	6 m	1.3 h	28 m
20News (20 classes)	7 m	2 m	5.4 h	2.0 h

## C Comparing foundation model embeddings to TabICL’s training data

We aim to study why PCA helps TabICL perform better on embeddings from frozen backbones. To do this, we create a stratified-by-class 100K subset of the iNaturalist dataset defined in Section A.7 and evaluate performance across a range of PCA dimensions, alongside effective rank and explained variance, shown in Figure 7. We only use DinoV3 features for this experiment, no tabular data.

We observe accuracy gains from PCA up to 64-dimensional embeddings, after which performance degrades as the latent becomes over-compressed at 32 and 16 dimensions. The curve plotting the product of explained variance and effective rank closely mirrors the accuracy curve, suggesting a tradeoff between preserving information in the latents and accommodating TabICL’s preference for high-effective-rank embeddings.

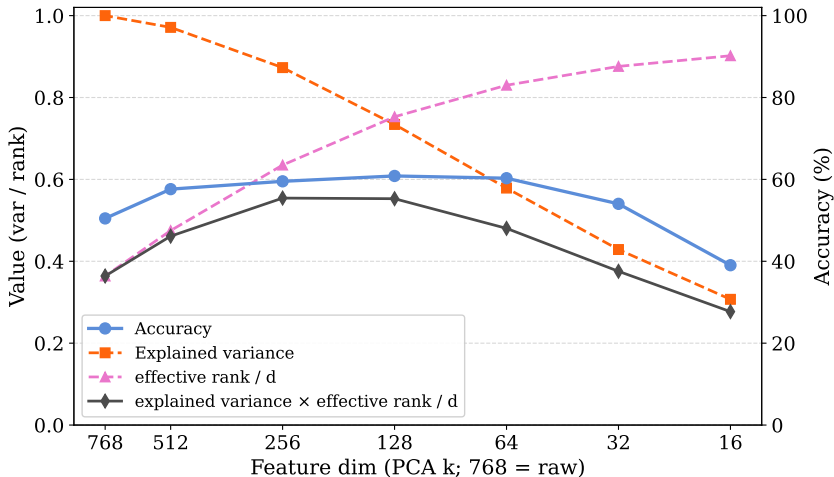


Figure 7: Explained variance, normalized effective rank and their product on subsampled iNaturalist across PCA dims.

We hypothesize that PCA helps because of a distribution shift between the synthetic data TabICLv2 was pretrained on and the embeddings produced by modality-specific backbones. To test this, we sample 20,000 datasets that approximate TabICL’s pretraining distribution and compare them to the iNaturalist embeddings actually fed into the model.

The TabICLv2 paper introduces a richer prior than TabICLv1, combining eight families of random functions with a new graph-sampling mechanism. However, the implementation of this v2 prior has not yet been publicly released. Only the v1 generators, which contain a mixture of MLP-based and tree-ensemble structural causal models are available. We therefore sample from the v1 generators while matching the curriculum schedule described in the v2 paper: dataset sizes are drawn across three stages (1,024 samples fixed; 400–10,240 log-uniform; and 400–60,000 log-uniform) in proportion to the published v2 training-step counts ( $\approx 91\%/7\%/2\%$ ). This provides the closest publicly available approximation to the distribution TabICLv2 encounters during pretraining.

Figure 8 compares iNaturalist embeddings against these synthetic samples. The embeddings seen during TabICLv2 pretraining are mostly isotropic, with more than 60% of samples exhibiting effective-ranks above 0.90. In contrast, raw DINOv3 CLS embeddings lie in the left tail of the prior’s distribution, having lower effective rank. Applying PCA gradually shifts the DINOv3 embeddings toward the bulk of the prior distribution. This suggests that the gains from PCA arise because TabICL is biased toward high-effective-rank embeddings, reflecting the statistical structure of its synthetic pretraining distribution.

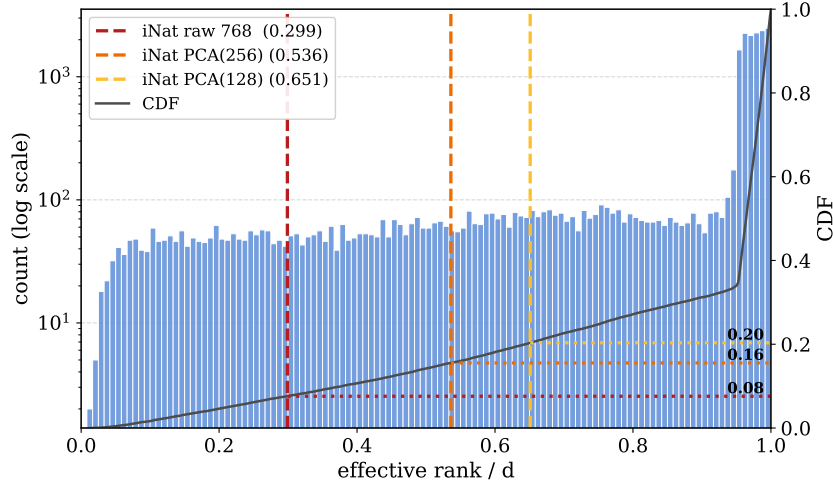


Figure 8: Comparing normalized effective rank between samples from TabICL’s prior to iNaturalist DinoV3 CLS tokens with various PCA settings. The log CDF of the histogram is shown in black, highlighting the distribution of the TabICL dataset’s effective ranks

## D Additional Results

### D.1 Impact of PCA dimensionality

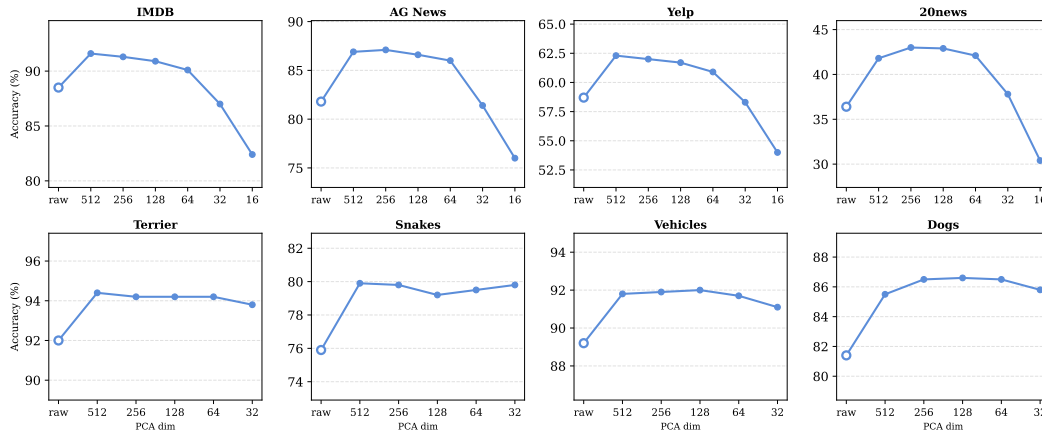


Figure 9: TabICL with varying PCA settings on a image and text only datasets. We find that even applying a slight amount of PCA results in a significant performance boost. PCA dimensions of 512, 256 and 128 are viable. Hence, in this paper, we either use PCA dims 256 or 128 in all experiments.

### D.2 Testing CoMET with different backbones

We also run CoMET on Franca Venkataramanan et al. (2025) for image encoding and RoBERTa Liu et al. (2019) for text encoding, shown in 14. Our results on different backbones show that our method is not limited to DinoV3 and ELECTRA, and that the benefits of PCA are due to TabICL, not the backbones.

Table 14: Results across a few multimodal and single modality datasets for RoBERTa and Franca.

<b>Dataset / Modality</b>	<b>Raw</b>	<b>PCA-256</b>
PetFinder (tabular + franca)	0.3730	<b>0.3991</b>
PetFinder (tabular + roberta)	0.4057	<b>0.4305</b>
PetFinder (tabular + franca + roberta)	0.3648	<b>0.4395</b>
MM-IMDb (franca)	0.5487	<b>0.5499</b>
MM-IMDb (roberta)	0.6538	<b>0.6574</b>
MM-IMDb (franca + roberta)	0.6495	<b>0.6607</b>
Airbnb-TTT (tabular + roberta)	0.4128	<b>0.4563</b>
Snakes (franca)	0.7212	<b>0.7576</b>
Vehicles (franca)	0.8705	<b>0.8732</b>

### D.3 PALPooling

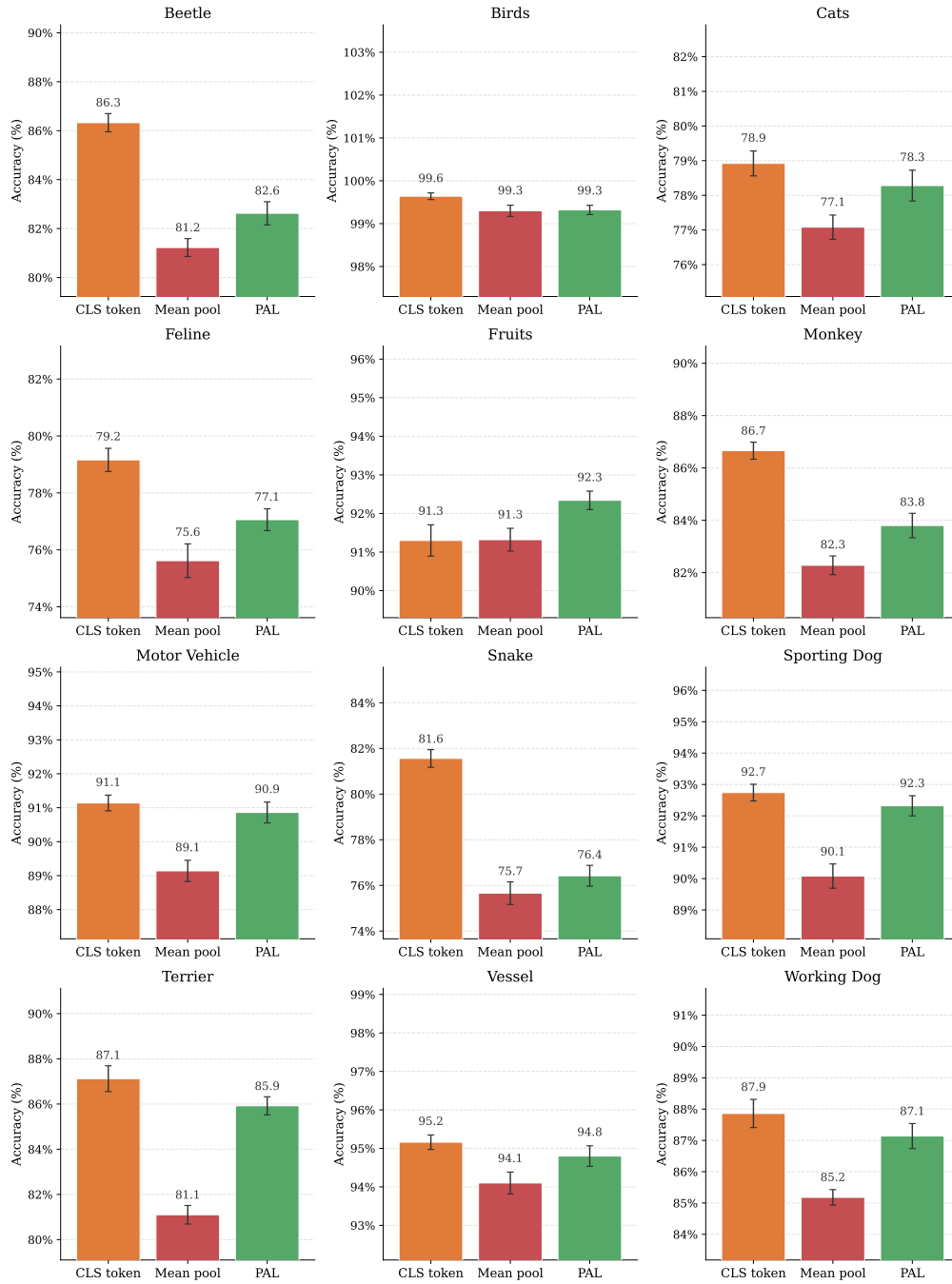


Figure 10: Performance of PALPooling for imagenet subsets where we expect the CLS-token to be strong. Still, we see PALPooling consistently improve over mean-pooling, which is the starting point of the algorithm.

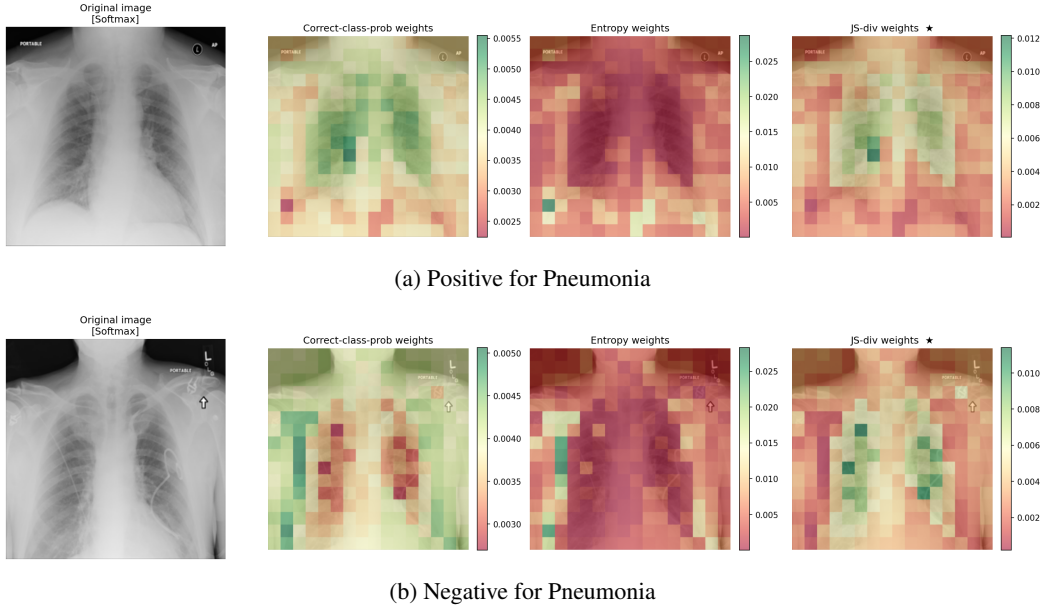


Figure 11: A comparison of different methods for generating PALs for RSNA-Pneumonia, where the lungs are the area of interest. While the correct-class probabilities work well for the positive case, it explicitly down-weights the lungs for negative samples. In the third column, we show the results when weights are derived from Shannon’s entropy on the predicted label distribution, down-weighting tokens that are closer to 50/50. We see that this approach does not work well for this dataset, likely because the label balance is close to 80/20%. This means that a piece of background could have a sharper (negative) prediction, compared to a piece of lung tissue. The right-most column shows the weights derived from the JS divergence between the token predictions and the prior label frequency. We see that the lungs are clearly highlighted, indicating that the token predictions are distinct from the class prior.

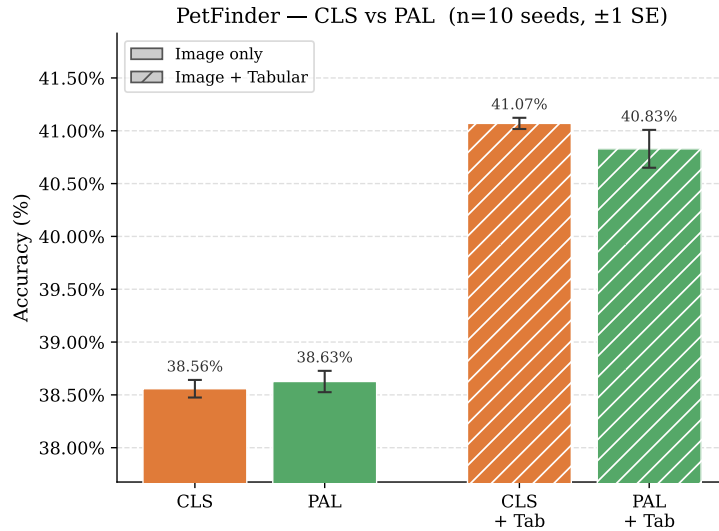


Figure 12: Example of when modality-agnostic pooling can become detrimental. The experiments are averaged over 10 seeds with error bars corresponding to 1 standard error. Experiments used a PCA dimension of 256 and 4 estimators in the TabICL model. Although we observe PALPooling perform similarly or better than the CLS token on the image-only task, we see that it has noticeably worse image + tabular performance.

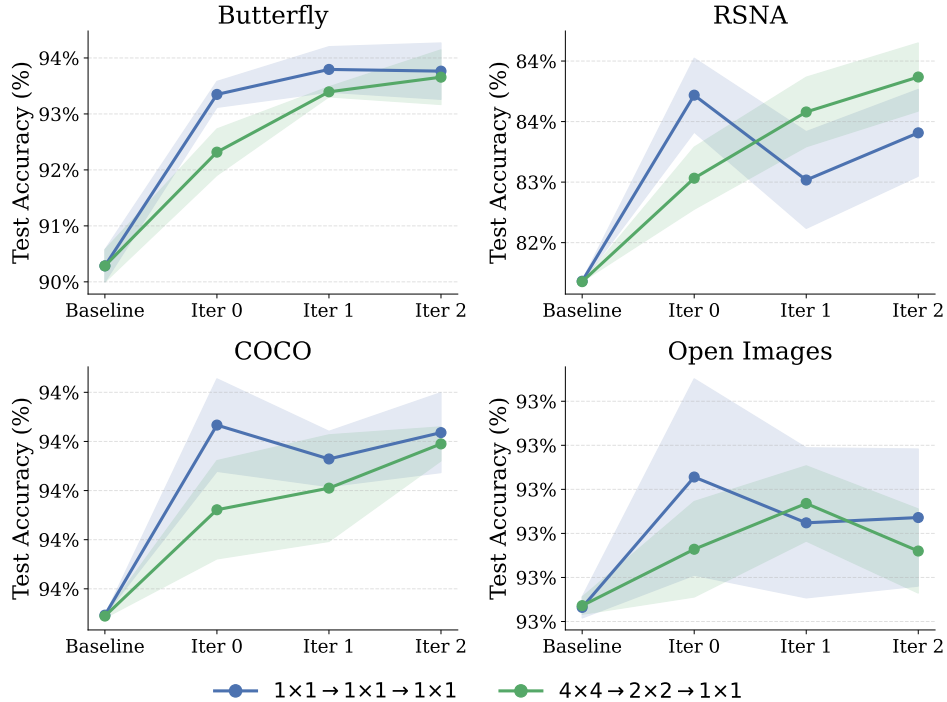


Figure 13: The impact of running PALPooling iteratively across the image datasets, as well as the choice effects of applying coarser pooling.

## D.4 Hierarchical classification

### D.4.1 Timing TabICL on Inaturalist

In Table 15, we compare the inference times of hierarchical and flat TabICL on iNaturalist under different sample caps. We find that training a hierarchical classifier with a cap of 100k–200k samples per TabICL fit is significantly faster than a flat TabICL classifier over all 2,896 classes, even when both use the same overall budget of 100k–200k samples.

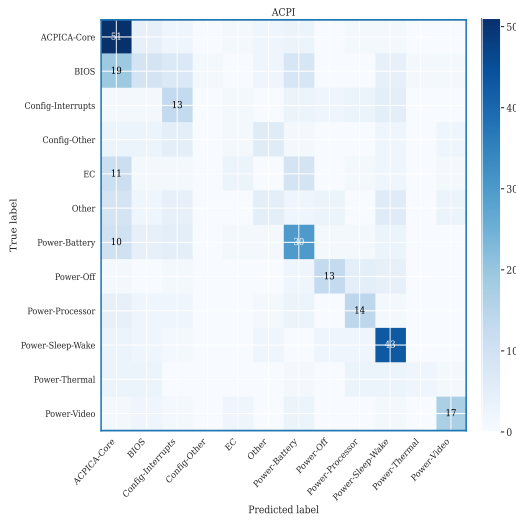
This improvement in speed/performance arises because the hierarchy decomposes the task into more manageable sub-problems for TabICL. The speedups stem from the use of mixed-radix ensembling in TabICL to handle more than 10 classes, which forces the flat baseline to perform significantly more forward passes as the number of classes increase. While the hierarchical model still performs forward passes with up to 200k context near the root of the tree, it operates over far fewer classes per TabICL fit than the flat approach, resulting in speed gains.

Table 15: Inference (predict) time on Naturalist (2,896 classes, 28,960 val images, mean (std) over 5 seeds, seconds).

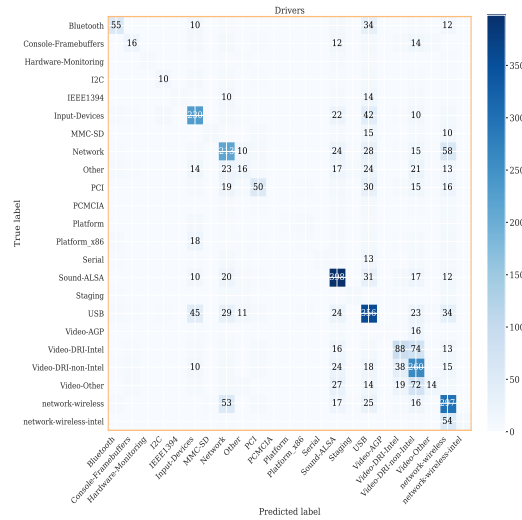
Model	Acc $\uparrow$	Predict time (s) $\downarrow$
H-CoMET (cap=100K)	82.24 (0.11)	227.1 (1.1)
H-CoMET (cap=200K)	82.50 (0.04)	315.1 (0.6)
F-CoMET ( $n=100K$ )	65.08 (0.24)	704.9 (1.7)
F-CoMET ( $n=200K$ )	69.54 (0.23)	1,464.4 (2.6)

### D.4.2 Text Benchmarks

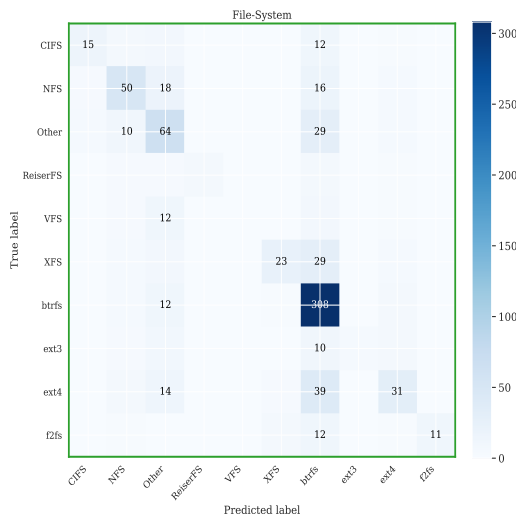




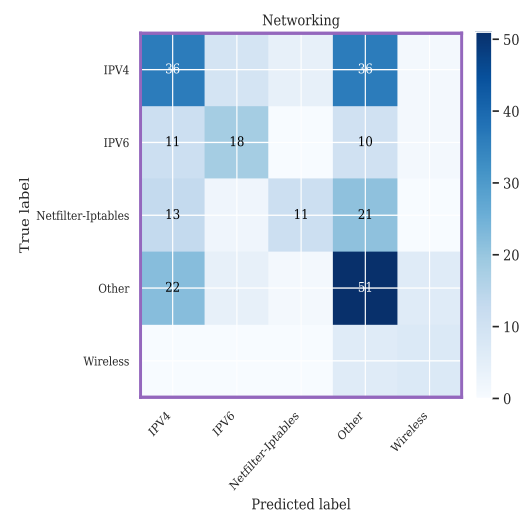
(a) TabICL-Flat ACPI Prediction



(b) TabICL-Flat Drivers Prediction

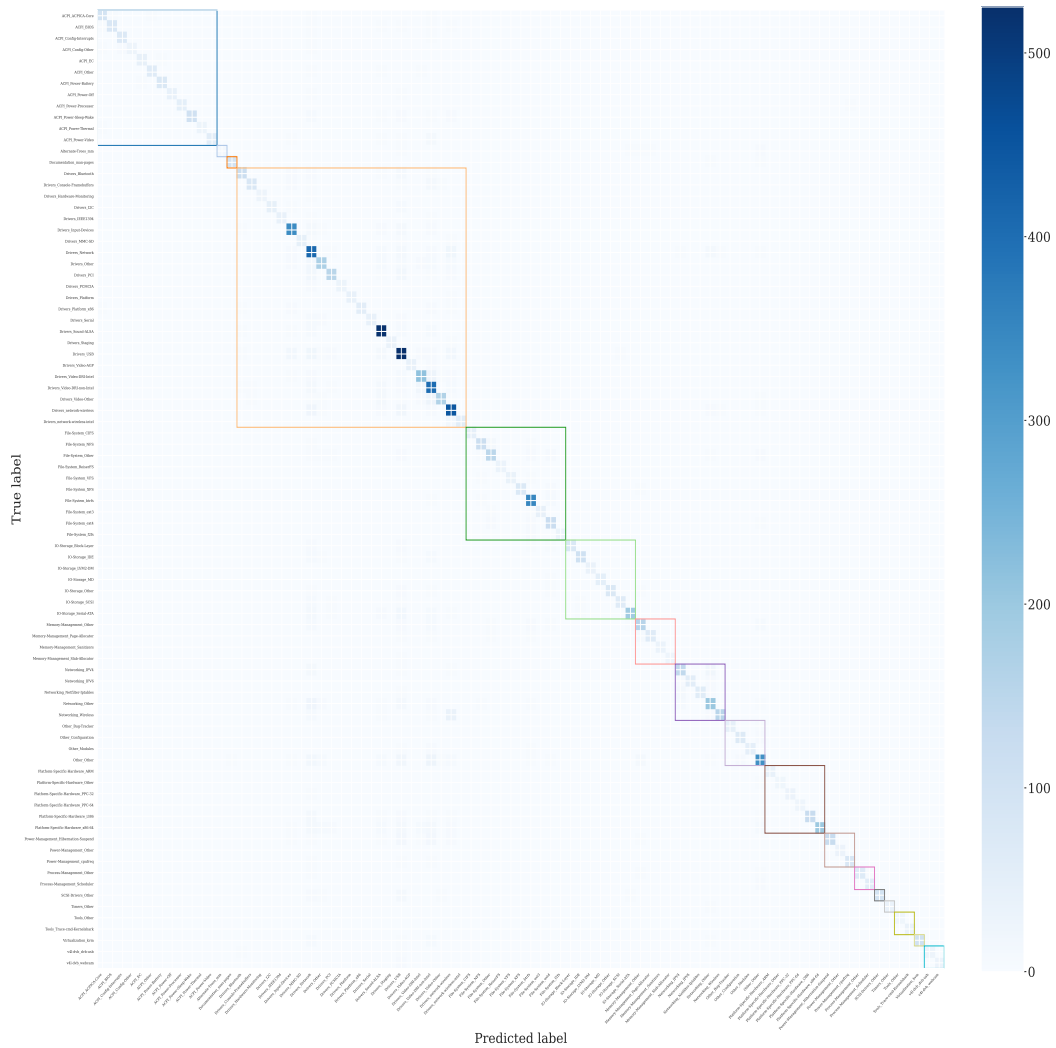


(c) TabICL-Flat File-System Predictions



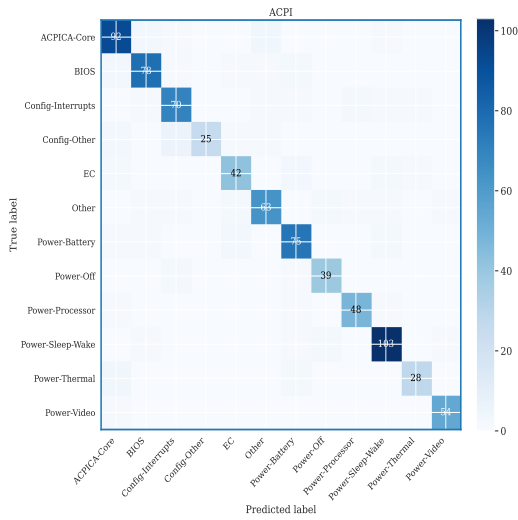
(d) TabICL-Flat Networking Predictions

Figure 15: Subcategory confusion matrices for TabICL-Flat on the Bugs dataset.

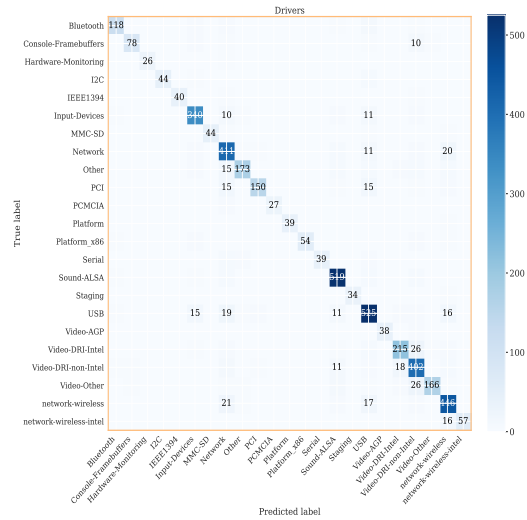


(a) Original

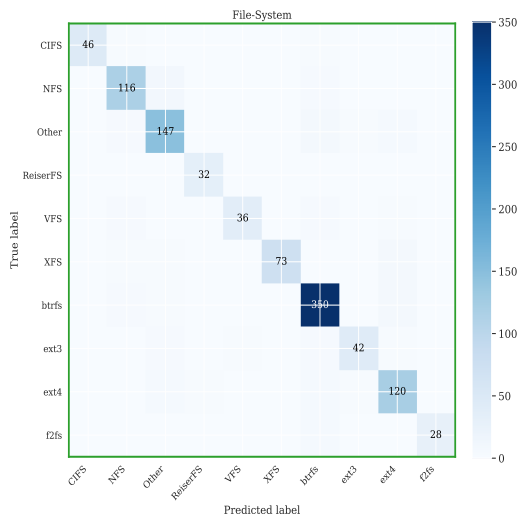
Figure 16: Overview confusion matrix for TabICL-Hierarchical on the Bugs dataset. Coloured blocks represent subcategories, a selection of which are shown in Figure 17.



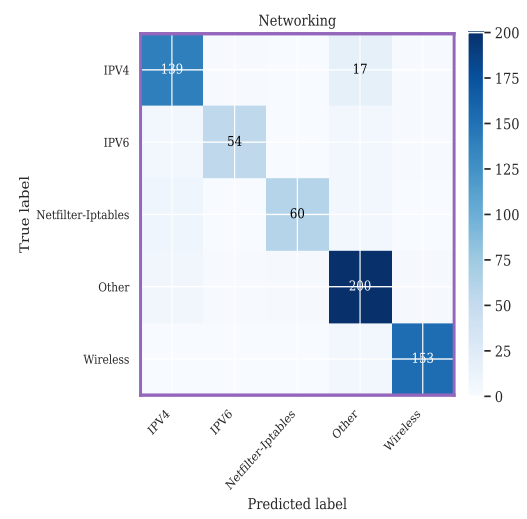
(a) TabICL-Hierarchical ACPI Prediction



(b) TabICL-Hierarchical Drivers Prediction



(c) TabICL-Hierarchical File-System Predictions



(d) TabICL-Hierarchical Networking Predictions

Figure 17: Subcategory confusion matrices for TabICL-Hierarchical on the Bugs dataset.